INSTITUTE FOR AEROSPACE STUDIES

UNIVERSITY OF TORONTO

AD 671122

THE EFFECTS OF SPECIMEN GRAIN SIZE AND ENVIRONMENT ON THE FATIGUE LIFE OF OFHC COPPER

by

W. Knapp

D D C

JUL

UTIAS

JUNE 1968

UTIAS TECHNICAL NOTE NO. 124

61

THE EFFECTS OF SPECIMEN GRAIN SIZE AND ENVIRONMENT ON THE FATIGUE LIFE OF OFHC COPPER

by

W. Knapp

Manuscript received March 1968

JUNE 1968

UTIAS TECHNICAL NOTE NO. 124

ACKNOWLEDGEMENTS

The author is indebted to Dr. G. N. Patterson, Director of the University of Toronto Institute for Aerospace Studies, for providing the opportunity to work on this project, and to Dr. G. K. Korbacher for initiating this project and for his interest in the progress of the work.

The author also wishes to thank Prof. W. A. Wood, Columbia University, for critically reading the manuscript and for his many helpful comments.

The help given to the author by Mr. W. Hoppe, Metallurgist, De Havilland Aircraft of Canada, Limited, and by Mr. R. Puccini is gratefully acknowledged.

This research project was supported financially by the National Research Council of Canada.

SUMMARY

This note presents the results of a study of the effects of grain size and environment on the fatigue life of OFHC copper specimens.

Tests conducted in alternating torsion on specimens of two different grain size groups showed that an increase in specimen grain size results in a decrease in fatigue life at both high and low strain amplitudes. Similar tests under low and high humidity showed that humidity has a negligible effect on fatigue life for either high or low strain amplitude and for large or small grain size. The effects of elevated temperatures were found to be more complex. At high strain amplitudes the fatigue life decreased continuously as the temperature was increased. At low amplitudes the life dropped as the temperature was raised to 200°C., but then remained approximately constant when the temperature was raised further to 350°C.

An examination of the microstructural changes caused by the fatigue tests revealed damage characteristics of Wood's H range for the tests at high amplitudes and room temperature, with slight variations for the tests at high temperature. Damage characteristics of Wood's S range were found for low amplitude tests at room temperature, with significant grain growth occuring at high temperature.

TABLE OF CONTENTS

INTRODUCTION

In the first half of this century the research done in fatigue of metals was focused primarily on the determination of the S (stress)-N(number of cycles to failure) characteristic of metals of practical interest. Usually a single specimen was broken at each stress level for a number of stress levels to determine this so-called S-N curve.

In the second half of this century, when it was finally recognized that fatigue is a statistical phenomenon, the determination of S-N curves has become more elaborate and precise, a result of replacing the single specimen fatigue test per stress level by statistically meaningful numbers of specimens at each stress level. For instance, in 1953, G.M. Sinclair and T.J.Dolan (Ref. 1) obtained significant results on the fatigue life of 75S-T6 Aluminum Alloy which clearly demonstrate the importance of applying statistical methods to fatigue testing. In 1960, S.R. Swanson (Ref. 2) of UTIAS published a report on the statistical fatigue properties of 2024-T4 aluminum alloy and in 1967 P.J. Haagensen (Ref. 3) of UTIAS investigated the statistical endurance distributions of OFHC copper specimens.

Also in recent years, the metallographic study of fatigued specimens has become an important part of fatigue research. This field was pioneered by W.A. Wood. He and H.M. Bendler found (Ref. 4) in 1962, that the S-N curve could be divided into three strain amplitude ranges, H, F and S, each of which is based on a characteristic type of fatigue failure mechanism. Many reports have been published furthering this principle. The most recent is a report by D. B. Muggeridge of UTIAS (Ref. 5) relating Wood's fatigue mechanisms to the S-N curve found by P.J. Haagensen (Ref. 3).

Now that some work has been done on the determination of more accurate S-N curves and their underlying fatigue failure mechanisms, attention is being turned to the effects of varying inherent and environmental parameters on the fatigue life of metals.

Work has been done by W. A. Wood and H.M. Bendler (Ref. 6) on the effect of superimposed static tension on the fatigue process in copper being subjected to alternating torsion and by M. Ronay, W.H. Reimann, and W. A. Wood (Ref. 7) on the effect of elevated temperatures on the fatigue life of 70-30 Brass. Studies by D. Hull (Ref. 8) and by D. L. Holt and W.A. Backofen (Ref. 9) explored the fatigue failure at low temperatures. The observed general trend of all this work is that the fatigue life decreases continuously with increasing temperatures.

As to the effect of grain size on metal fatigue behaviour, reports have been published by R. W. Karry and T.J. Dolan (Ref. 10) and by P.G. Forrest (Ref. 11) which show in general a decrease in fatigue life with increasing grain size.

The effects of atmospheric corrosion on fatigue life were investigated by N.J. Wadsworth and J. Hutchings (Ref. 12). They found, for electrolytic tough pitch copper with a very large grain size (0.5 mm.D), that high humidity has a negligible effect upon fatigue life.

With these foregoing facts in mind, this report was prepared. Ten specimens were tested at each test specification to give a reliable estimate of the mean fatigue life under given conditions. Then, a metallographic examination was made of one of these ten specimens to correlate fatigue life and fatigue mechanisms. Altogether, two grain sizes were tested at two strain amplitude levels for three temperatures and two relative humidity levels.

I. TEST EQUIPMENT, SPECIMEN PREPARATION, AND TEST PROCEDURE

1.1 Test Equipment

1.1.1 Fatigue Machine

The basic fatigue machine (Fig. 1) developed by Prof. W. A. Wood, was purchased from Columbia University, New York. It fatigues single specimens under alternating torsional loading. A mechanical counter is used to record the specimen lives in cycles. Provision is made, by means of an end carriage (Fig. 2), stiff in the torsional but free-moving in the axial direction, for static axial tensile load applications.

An automatic shut-down device (Fig. 3) was developed at UTIAS. It is based on the principle that the specimen becomes elongated as the macro-crack forms, and a transducer (Fig. 4) is used to detect this elongation. The signal from the transducer is fed to the controller (seen in Fig. 3) which shuts down the machine.

1.1.2 Humidity Control Chamber

The humidity control unit (see Figures 5 and 6) produced, in the small plastic chamber around the specimen, a controlled relative humidity between 10% and 70% with a tolerance of ± 1½% at 27°C. A manual control provided humidities above 70%. The temperature at 27°C is controlled within ± 1 C°.

1.1.3 Specimen Heater

A specimen heater unit (Figures 7 and 8) permitted the performance of fatigue testing at elevated temperatures. A miniature thermocouple and a controller (Fig. 9) were used to control the specimen temperature during testing to ± 5°C with a temperature cycling period of about 2 minutes.

1.2 Specimen Preparation

1.2.1 Material

The material selected for these experiments was OFHC copper. The specifications of this copper are:

Copper	99.96 percent by weight min.
Phosphorous	less than 0.003 percent
Sulphur	less than 0.0040 percent
Zinc	less than 0.0003 percent
Mercury	less than 0.0001 percent
Lead	less than 0.0010 percent

This copper was purchased in the form of rods of 5/16" diameter, 6' length, in the 1/2 hard, cold drawn condition.

The grain structure of the copper as received is shown in Fig. 10. The deformed grains illustrate the work-hardened state of the material, which is also illustrated by a back-reflection X-ray photograph shown as Fig. 11.

In Table I, the Diamond Pyramid Hardness test results (136° Diamond) for this material are recorded to be about 120. The static tensile properties are also given in Table 1.

1.2.2 Machining and Mechanical Polish

The test specimens were machined, on a small lathe, from the 5/16 inch dia. rod. The final dimensions are shown in Fig. 12. A ½" Radius tool was used to make the final cuts to the given dimensions.

After they were machined, the specimens were polished mechanically on a small lathe. First they were polished with 3/0 grit emergy paper, and then with 4/0 grit emery paper, both lubricated with varsol, to remove the machining marks.

1.2.3 Annealing

The machined and polished specimens were then annealed in groups of 10 in a small annealing oven (Fig. 13). Further information on the oven is given in Appendix A.

A continuous nitrogen cross-flow of 5 cubic feet per hour through the oven chamber was used during heating and cooling.

The details of the heat treatments applied in order to produce specimens of small and large grain sizes are as follows:

a) Small Grain Size (Group A)

The specimens in this group were heated to a temperature of 1150°F and held at that temperature for 45 minutes. The heating and cooling curve is shown in Fig. 14. The average heating rate is 382F° per hour. The average cooling rate, between 1150°F and 600°F, is 147F° per hour, and the average cooling rate between 600°F and 200°F is 61F° per hour.

The resultant small grain structure is shown in Fig. 15. This photo and Fig. 19, depicting the large grain structure, were taken of an area at the specimen axis on a longitudinal section as shown in Fig. 17. A back-reflection X-ray photograph of the small grain structure is given in Fig. 16. It proves that the material is annealed, as compared with the cold-drawn material shown in the X-ray of Fig. 11. Also, the large number of clear spots shows that the grain size is fairly small

The grain structure shown in Fig. 15 shows very clearly the annealed state of the material. It is to be noted that there is quite heavy twinning in the structure, and that this twinning tends to orient itself in the axial direction of the specimen. This occurs to relieve the stresses created by drawing the copper in the axial direction during manufacture. It is also obvious from Fig. 15 that the grains are non-uniform in a manner to be expected if recrystallization were incomplete

The tensile properties of this annealed material are given in Table I. It is seen that the hardness of the metal has dropped to about 40 as compared to 120 for the cold-drawn rod. Also, the ultimate tensile strength and the 0.1% proof strength have dropped, and the % elongation at fracture has become larger. These facts are further proof of the annealed state of the annealed state of the material.

The grain size of the copper after annealing was determined by comparison with ASTM grain size charts. Small areas were chosen along the specimen axis and along lines perpendicular to the axis at each end and in the centre of the longitudinal section shown in Fig. 17. Areas were also chosen along two perpendicular lines in each of the two cross-sections. The grain sizes in these areas were then estimated, and then averaged to give the specimen average grain size. The range of grain sizes was noted and is commented on if there was a large variation. This procedure was repeated for five specimens of each group and averages taken to give a group average grain size. It was found that the grain size did not vary appreciably from specimen to specimen within the groups.

The average grain diameter of the group A specimens was found to be 0.034 mm.

b) <u>Large Grain Size (Group B)</u>

The specimens in this group were heated to a temperature 1600°F and held at that temperature for five minutes. The heating and cooling curve is shown in Fig. 18. The average heating rate between 100°F and 1150°F is 500 F° per hour, and the average heating rate between 1150°F and 1600°F is 92 F° per hour. The average cooling rate between 1600°F and 1150°F is 318F° per hour, the rate between 1150°F and 600°F is 151F° per hour, and the rate between 600°F and 200°F is 58F° per hour.

The resultant grain structure at an area on the specimen axis (See Fig. 17) is shown in Fig. 19. A back-reflection X-ray photograph of this same structure is given in Fig. 20.

From the X-ray photo (Fig. 20) it follows that the copper is again annealed and the small number of clear spots indicates that the grain size is relatively large.

From the grain structure shown in Fig. 19, the grain size is indeed quite large. Again there is fairly heavy twinning, tending to the axial direction, thus indicating an annealed metal.

The tensile properties of this annealed material are given in Table I. Again it was found that the hardness of the metal has dropped to about 35 as compared to 120 for the cold-drawn rod. The ultimate tensile strength and 0.1% proof strength have dropped, and the % elongation at fracture is also larger. Again, these facts inilicate annealing.

An interesting fact found during the tensile tests was that the cold-drawn rod and the small grain specimens all failed with a double-cup fracture, while the large grain size specimens failed with a shear fracture at 45° to the specimen axis. It appears that in the large grain size group the final failure occurs by slip within a single grain.

A fairly large variation in grain size was found in this group with the average grain diameter being 0.19 mm.

1.2.4 Electro-Polishing

After annealing, the specimens were electro-polished in a bath of 2 parts O-phosphoric acid and 1 part distilled water at 2.1 volts for 20 minutes. This procedure removed 0.0005" from the surface of the specimen, thus reducing the diameter by 0.001", and leaving a very smooth surface. The specimens were then ready for testing.

1.3 Test Procedure

Before the start of a test, the driving arm of the torsion machine is set at zero angle of deflection by means of a dial gauge (Fig. 21) measuring in thousandths of an inch. The specimen is then clamped in the grips (Fig. 1) for testing. The dial gauge is also used to measure the amplitude of the arc of motion of the driving arm and thus to determine the strain amplitude at which the specimen is being tested.

For the tests under room conditions and under controlled humidity, the transducer (Figs. 3 and 4) is then given an initial deflection by means of the micrometer. This deflection produces a voltage reading (usually set at 0.5 volts) on the controller. The machine is then started. The voltage reading on the controller remains constant until the specimen starts to fail. At that point the controller turns on a small solenoid (Fig. 3). This solenoid pulls the breaking specimen apart more rapidly, and the machine shuts down when failure is complete. The life, N, of the specimen in cycles is then recorded by the mechanical counter.

For the tests under controlled high temperature conditions, it was found that the fatigue life of the specimens could be measured more accurately by applying a constant tensile load of 645 psi to the specimen with the device shown in Fig. 2. Again the specimen was clamped in the grips and then heated to the test temperature (either 200°C or 350°C). The elongation of the specimen due to the added heat was recorded, and when an equilibrium length was reached it was assumed that the specimen had reached thermal equilibrium.

The fatigue test was then started, and the further creep of the specimen was recorded. A typical creep curve is shown in Fig. 22. From these curves, the final fracture point could easily be predicted.

The tensile load used in these temperature tests was small enough that it would not affect the life of the specimen significantly. This view is supported by the work of Wood and Bendler in Ref. 5.

II. FATIGUE TEST RESULTS

2.1 Fatigue Life Results

From each of the two grain size groups, 50 specimens were to be tested at low amplitude ($\pm$ 2.0 deg. torsional fatigue) and 50 specimens at high amplitude ($\pm$ 10.0 deg. torsional fatigue).

Each of these 4 bunches of 50 specimens was then divided into 5 batches of 10 specimens each and out of each of the 4 bunches, one batch was tested under room conditions of random temperature and humidity, the next with temperature and humidity controlled at the average temperature (27°C) and humidity experienced by the batch tested previously under room conditions. The third batch followed then with temperature controlled at 27°C and humidity held at 100%, the fourth with temperature controlled at 200°C and the last batch with temperature controlled at 350°C.

For each of these 20 batches of 10 specimens the fatigue endurances are listed in Table II, from which the mean fatigue lives, $\overline{N}$, in cycles were calculated and tabulated in Table III for the parameters, grain size, shear strain amplitude, and test temperature and humidity (relative) of each batch.

The fatigue life results thus found are plotted on Figs. 23 - 28. The results for similar test conditions (e.g. 27°C, 100%) at both test strain amplitudes ($\pm$ 2.0°, $\pm$ 10.0°) are plotted on a graph of strain amplitude (in degrees) versus fatigue life, N, in cycles. It should be noted that for the specimen diameter used, 1° of torsional twist corresponds to 0.0015 surface shear strain. Thus the specimens tested at $\pm$ 2.0 degrees are subjected to $\pm$ 0.003 surface shear strain, and the specimens tested at $\pm$ 10.0 degrees are subjected to $\pm$ 0.015 surface shear strain.

Although the test results plotted on these figures are known only for test amplitudes of 2.0 degrees and 10.0 degrees, the test results for other amplitudes can be estimated roughly. Such an estimate is based on the slopes of the straight line portions of the S-N curve, the H-(high stress, short life) range part and the S-(low stress, long life) range part, taken as those found by Wood and Bendler (Ref. 4, p. 183), in tests on OFHC copper in torsional fatigue. However, the curved transformation region of the F-range as found by Wood and Bendler, has been replaced by a sharp knee, which is considered to be permissible, since the S-N curve is for comparative purposes only.

The results at room conditions and controlled (low and high) humidity of the small grain specimens (Group A) are plotted in Fig. 23. It is seen that the test humidity has a negligible effect on the fatigue life. Therefore only a single S-N curve was drawn through the means of each of the high and low amplitude lives. In Fig. 24, a similar result is found for the effect of humidity on the lives of the large grain (Group B) specimens. Again only a single S-N curve was drawn. In Fig. 25, the effect of elevated temperature upon the lives of the Group A specimens is shown. As expected from the results of previous authors, the specimen lives at high amplitude decrease progressively as the test temperature is raised. However, in the low amplitude ($\pm$ 2.0 deg. - S-Range) tests, the specimen lives decreased sharply when the temperature was raised to 200°C, and then remained effectively the same as the temperature was raised further to 350°C. In Fig. 26, a similar result is found for the effect of temperature on the lives of the Group B specimens. The decrease in fatigue life with temperature is further shown in Fig. 28. The log of the mean fatigue life, $\bar{N}$, decreases linearly with increasing temperature at high amplitude fatigue testing. However, at low amplitude the decrease is discontinuous, and the life is approximately constant above 200°C.

In Fig. 27, the effect of the change in grain size is shown for the tests at room temperature. These points were found by averaging the fatigue lives for the random, the controlled low, and the controlled high humidity tests. It is seen that the increase in grain size causes a definite decrease in fatigue life at low and high strain amplitudes.

These results are well confirmed by those of other researchers. As mentioned before, Wadsworth and Hutchings (Ref. 12) also found that high humidity has a negligible effect on the fatigue life of a similar material, electrolytic tough pitch copper. Also, the results found by W.A. Wood, M. Ronay, and W.H. Reimann (Ref. 7) of the effects of elevated temperatures on the fatigue life of 70-30 Brass at intermediate and high strain amplitudes are very similar to the results found in our tests at high amplitudes and elevated temperatures.

2.2 Microstructure Examination

After the fatigue tests were completed, 20 specimens, one from each batch, were selected and silverplated. From the specimens tested at low amplitude, the one from each batch with the longest life was selected. For specimens tested at high amplitude, the one with the shortest life was selected from each batch.

These silverplated specimens were then mounted in plastic and sectioned, as shown in Fig. 29, for an examination of the microstructure after fatigue.

The type of failure occuring in the specimens of batches 1, 2 and 3 (see Table III) is seen from Figs. 30, 31 and 32 to be the same as that found by other researchers for low amplitude fatigue. It is primarily that of the S-range found by Wood and Bendler. That is, there are many cracks occuring mainly along grain boundaries. There is also some slip occuring but there are few slip zone concentrations. Examples of the notch-peak effect found by Wood are seen in Figs. 30 and 31.

In the temperature tests at 200°C (batch 4), the microstructure as shown in Fig. 33 indicates that the cracking is still primarily of the grain boundary type, with some rectangular cracking appearing.

In the specimens of batch 5 tested at 350°C, it is found that grain growth and boundary migration has taken place in the material, as shown in Figs. 34 and 35. The grain boundaries after migration have a tendency to orient themselves perpendicular and parallel to the specimen axis. Again cracking is mainly grain boundary type with some rectangular transgranular cracks. The slip is now present only at the surface as shown in Fig. 35.

The tests on the large grain size specimens of batches 6, 7, and 8 again resulted in an S-type structure as shown in Figs. 36, 37, and 38. As seen in Figures 36 and 38, there is more fine slip than seen with the small grain size specimens, but the cracking occurs still mainly along grain boundaries. The low amplitude effect is also demonstrated in Fig. 37, where the twins remained straight.

In the tests on batch 9 at 200°C, the cracking again remains mainly along grain boundaries as shown in Fig. 39. The tests on batch 10 at 350°C again reveal grain growth and boundary migration (compare with small grain size case, Figs. 34 and 35). In this specimen, shown in Figure 40, it is seen that cracking again proceeds along grain boundaries, and some twin boundaries, and that only a small amount of slip is still present.

High amplitude tests were conducted on the specimen batches 11 to 20. Of these, batches 11 to 15 were of small grain size and batches 16 to 20 were of large grain size.

The failures in batches 11, 12 and 13 were of the same type. Features of this failure are shown in Figs. 41, 42 and 43. An area distant from the final fracture is seen in Fig. 41. The cracks proceed along grain boundaries. The structure is distorted as seen by the bent twins. The notch-peak effect is no longer present, as seen by the surface area shown at 1000X in Fig. 42. At an area near the final fracture, shown in Fig. 43, the cracking becomes rectangular, and the structure is badly distorted and has developed a sub-grain or cell structure characteristic of the large-amplitude H mechanism.

In the temperature tests at 200°C on batch 14, the cracking is again rectangular, as seen in Fig. 44, and the structure is distorted. The temperature tests at 350°C on batch 15 again produced a badly distorted structure and rectangular cracking (Fig. 45). It should also be noted that grain growth has not occurred in these high temperature tests. This might possibly be due to the very short testing times involved at high amplitudes and the obstructions produced by cracks.

The high amplitude tests on large grains (batches 16, 17 and 18) again produced similar results as those observed with the small grain specimens. Examples of the damage produced are shown in Figs. 46, 47, and 48. The results are in general badly distorted structures and many cracks.

The temperature tests at 200°C on batch 19 also produced badly distorted structures with rectangular type cracking as exemplified in Fig. 49. In the tests at 350°C on batch 20, grain boundary migration appears to have occurred with rectangularly oriented grains (parallel to and perpendicular to the specimen axis) as shown in Fig. 50. The cracking remains of a rectangular nature.

III. CONCLUSIONS

From the fatigue test results and the examination of the microstructure of fatigued OFHC copper specimens, it is apparent that:

(1) relative humidity (19.5% to 100%) has only a negligible effect on fatigue life. This observation applies to specimens of large (0.19 mm) or small (0.034 mm) grain size, fatigued at high (10°) or low (2°) strain amplitudes.

(2) increasing grain size from 0.034 to 0.19 mm reduces fatigue life at room temperature and

a) 2° strain amplitude by a factor of about 4, but at

b) 10°, very little

At elevated temperatures, fatigue life was found to reduce with grain size at

c) 2° strain amplitude by a factor of about 3 and at

d) 10° by only 10 to 20%

(3) the effects of temperature on fatigue life were not very pronounced but interesting insofar as at the

a) high strain amplitude (10°), the fatigue life dropped progressively as the temperature is raised from 20° to 350°C. However, at the

b) low strain amplitude (2°), the life dropped only from 20°C to 200°C, but then did not change as the temperature was further increased to 350°C. This behaviour suggests that the drop in fatigue life at the low strain amplitude may be entirely due to oxidation of the specimens. This point merits further research.

Another interesting feature of the high temperature fatigue at low amplitudes is the grain boundary migration leading to boundaries oriented in a direction parallel or perpendicular to the torsional shear stress. Whether this migration occurs to boundaries of the original grains or whether new grains also form is not clear.

REFERENCES

1. Sinclair, G.M. Dolan, T.J. — Effect of Stress Amplitude on Statistical Variability of Fatigue Life of 75 S-T6 Aluminum Alloy. Trans. Amer. Soc. Mech. Engrs - 75 (1953) p. 867.

2. Swanson, S.R. — Systematic Axial Load Fatigue Tests Using Unnotched Aluminum Alloy 2024-T4 Extruded Bar Specimens. UTIA TN 35, May 1960.

3. Haagensen, P.J. — Statistical Aspects of Coexisting Fatigue Failure Mechanisms in OFHC Copper. UTIAS TN 112, June 1967.

4. Wood, W.A. Bendler, H.M. — The Fatigue Process in Copper as Studied by Electron Metallography. Transactions of the Metallurgical Society of AIME-Vol. 224, Feb. 1962, p.180.

5. Muggeridge, D.B. — An Attempt to Correlate Bimodal Fatigue Endurance Distributions in OFHC Copper with Wood's H, F and S Ranges. UTIAS TN 111.

6. Wood, W.A. Bendler, H.M. — Effect of Superimposed Static Tension on the Fatigue Process in Copper Subjected to Alternating Torsion. Transactions of the Metallurgical Society of AIME - Vol. 224, (Feb. 1962), p. 18.

7. Ronay, M. Reimann, W.H. Wood, W.A. — Mechanism of Fatigue Deformation at Elevated Temperatures. Trans. Met. Soc. AIME, Feb. 1965.

8. Hull, D. — Surface Structure of Slip Bands on Copper Fatigued at 293°, 90°, 20°, and 4.2°K. J. Inst. Met., 86 (1958), p. 425-430.

9. Holt, D. L. Backofen, W.A. — Fatigue Fracture in Copper and the Cu-8 Wt Pct Al Alloy at Low Temperature. Trans. Met. Soc. of AIME, Vol. 239, Feb. 1967, p. 264.

10. Karry, R.W. Dolan, T.J. — Influence of Grain Size on Fatigue Notch Sensitivity. Proc. Amer. Soc. Test Mat. - 53 (1953), p. 789-804.

11. Forrest, P.G. — The Influence of Grain Size on the Fatigue Behavior of 70/30 Brass. J. Inst. Metals, Vol. 93 (1964-65), p. 438.

12. Wadsworth, N.J. Hutchings, J. — The Effect of Atmospheric Corrosion on Metal Fatigue.

APPENDIX A

Annealing Oven

An annealing oven (Fig. 13) was built to anneal specimens of the two groups.

A Thermovolt Controller was purchased to provide control from 60°F to 1600°F. A 240 volt A.C. power source was used with a control device to give control from 5 volts to 236 volts.

A resistive heater unit was made-up by wrapping wire around a refractive core. Vermiculite was used as insulation around the heater, and transite outer shielding was used.

A fitting was provided on one of the end plates for either a continuous nitrogen flush or for connection to a vacuum pump.

The specimens were laid on aluminum oxide packing in the stainless steel specimen tray. Two thermocouples were buried in the aluminum oxide with leads to the outside. One was used for control, the other one for recording.

TABLE I

CONTROL TENSILE SPECIMEN DATA

Specimen Number	Diameter (Mean) Inches	0.1% Proof Stress (psi)	Tensile Strength (psi)	$Ex10^{-6}$ (psi)	Elongation (%)	Area Reduction (%)	Diamond Pyramid Hardness of Unfatigued Material
TA1	0.2209	4,780	40,800	19.2	66.7	94.2	40.5
TA2	0.2217	5,050	40,700	17.5	61.7	93.7	39.6
TA3	0.2214	6,860	40,700	23.4	63.0	94.2	39.3
TA4	0.2212	4,910	40,800	12.8	63.0	94.0	39.0
TA5	0.2212	5,230	40,700	15.8	60.0	93.5	39.4
TB1	0.2204	3,170	41,800	16.7	42.7	100%	32.6
TB2	0.2215	4,280	42,800	17.3	44.8	100%	31.3
TB3	0.2210	2,840	43,100	15.6	46.7	100%	32.5
TB4	0.2210	3,020	41,800	17.0	40.8	100%	32.8
TB5	0.2211	3,620	42,300	14.1	42.0	100%	33.0
TO1	0.2212	58,600	71,900	25.8	18.7	86.8	118.7
TO2	0.2209	57,800	74,700	20.7	18.9	85.5	121.6
TO3	0.2210	59,100	74,700	19.2	16.9	86.8	121.2
TO4	0.2211	64,800	74,500	17.5	20.0	85.7	124.8
TO5	0.2215	56,300	74,100	20.4	20.2	87.9	125.3

TABLE II

RECORD OF THE FATIGUE TEST ENDURANCES

Batch No.	Specimen No.	Fatigue Life N (cycles)	Mean Life $\bar{N}$ (cycles)
1	A- 1	942,125	
	2	1,035,425	
	3	919,774	
	4	973,897	
	5	976,179	
	6	1,016,660	1,001,604
	7	1,047,270	
	8	1,030,455	
	9	1,027,818	
	10	1,046,445	
2	A-11	864,586	
	12	947,870	
	13	1,094,460	
	14	1,041,976	
	15	1,001,210	1,003,342
	16	984,536	
	17	1,146,100	
	18	1,045,834	
	19	983,795	
	20	923,055	
3	A-21	840,526	
	22	864,035	
	23	793,856	
	24	857,268	
	25	887,305	
	26	822,446	
	27	1,091,380	888,504
	28	901,800	
	29	965,400	
	30	861,020	
4	A-31	743,064	
	32	303,340	
	33	330,294	
	34	336,754	
	35	346,405	
	36	386,435	493,330
	37	398,910	
	38	342,706	
	39	506,863	
	40	1,238,530	
5	A-41	612,250	
	42	838,459	
	43	391,496	
	44	427,080	
	45	374,584	
	46	337,580	473,942
	47	541,739	
	48	395,455	
	49	317,124	

TABLE II
(continued)

Batch No.	Specimen No.	Fatigue Life N (cycles)	Mean Life $\bar{N}$ (cycles)
6	B- 1	314,884	
	2	214,900	
	3	207,029	
	4	256,577	
	5	256,304	
	6	244,181	235,754
	7	216,344	
	8	142,895	
	9	249,241	
	10	255,180	
7	B-11	354,471	
	12	222,694	
	13	412,215	
	14	296,881	
	15	298,661	
	16	255,832	
	17	261,895	285,715
	18	230,940	
	19	300,220	
	20	223,341	
8	B-21	288,083	
	22	282,794	
	23	260,736	
	24	172,197	
	25	340,940	
	26	248,063	265,239
	27	238,923	
	28	294,511	
	29	237,547	
	30	288,600	
9	B-31	113,409	
	32	138,406	
	33	144,344	
	34	166,450	
	35	119,925	
	36	119,671	
	37	133,538	140,369
	38	160,021	
	39	163,814	
	40	144,114	
10	B-41	108,735	
	42	143,440	
	43	176,603	
	44	176,385	
	45	149,975	
	46	167,615	157,459
	47	163,617	
	48	149,703	
	49	135,059	
	50	203,459	

TABLE II (continued)

Batch No.	Specimen No.	Fatigue Life N (cycles)	Mean Life $\bar{N}$ (cycles)
11	A-51	14,986	
	52	12,692	
	53	14,545	
	54	13,869	
	55	22,965	
	56	16,485	15,560
	57	14,482	
	58	13,415	
	59	18,159	
	60	14,000	
12	A-61	14,348	
	62	15,115	
	63	13,970	
	64	29,535	
	65	14,193	
	66	16,330	
	67	15,142	17,284
	68	15,440	
	69	15,810	
	70	22,960	
13	A-71	14,303	
	72	34,145	
	73	31,970	
	74	15,006	
	75	15,410	
	76	14,510	19,967
	77	19,775	
	78	21,285	
	79	16,315	
	80	16,955	
14	A-81	6,446	
	82	11,055	
	83	12,325	
	84	7,098	
	85	9,206	
	86	8,975	9,567
	87	13,495	
	88	8,310	
	89	10,833	
	90	7,390	
15	A-91	6,695	
	92	5,353	
	93	5,046	
	94	7,062	
	95	5,373	
	96	5,658	5,671
	97	6,145	
	98	5,605	
	99	5,301	
	100	5,370	

TABLE II (concluded)

Batch No.	Specimen No.	Fatigue Life N (cycles)	Mean Life $\bar{N}$ (cycles)
16	B-51	10,740	
	52	13,935	
	53	13,475	
	54	13,441	
	55	11,465	
	56	13,650	12,712
	57	9,580	
	58	11,860	
	59	16,565	
	60	12,412	
17	B-61	10,930	
	62	14,560	
	63	13,450	
	64	11,610	
	65	11,943	
	66	13,163	12,575
	67	10,580	
	68	14,230	
	69	12,670	
	70	12,620	
18	B-71	19,713	
	72	13,795	
	73	18,910	
	74	16,041	
	75	23,455	
	76	12,995	15,638
	77	8,665	
	78	14,525	
	79	14,080	
	80	14,200	
19	B-81	6,863	
	82	7,485	
	83	6,715	
	84	5,600	
	85	8,875	
	86	7,956	7,856
	87	9,351	
	88	8,010	
	89	8,762	
	90	9,140	
20	B-91	4,138	
	92	4,622	
	93	4,470	
	94	5,883	
	95	4,745	
	96	6,112	4,727
	97	3,800	
	98	4,770	
	99	4,960	
	100	3,770	

TABLE III

FATIGUE TEST RESULTS

Batch No.	Specimen Group	Grain Size	Test Amplitude ± degree	Test Temperature	Test Humidity %	Mean Fatigue Life $\bar{N}$ cycles
1	A	small	2.0	random	random	1,001,604
2	A	small	2.0	27°C	19.5	1,003,342
3	A	small	2.0	27°C	100	888,504
4	A	small	2.0	200°C	-	493,330
5	A	small	2.0	350°C	-	473,942
6	B	large	2.0	random	random	235,754
7	B	large	2.0	27°C	27.5	285,715
8	B	large	2.0	27°C	100	265,239
9	B	large	2.0	200°C	-	140,369
10	B	large	2.0	350°C	-	157,459
11	A	small	10.0	random	random	15,560
12	A	small	10.0	27°C	52.2	17,284
13	A	small	10.0	27°C	100	19,967
14	A	small	10.0	200°C	-	9,567
15	A	small	10.0	350°C	-	5,671
16	B	large	10.0	random	random	12,712
17	B	large	10.0	27°C	47.5	12,575
18	B	large	10.0	27°C	100	15,638
19	B	large	10.0	200°C	-	7,876
20	B	large	10.0	350°C	-	4,727

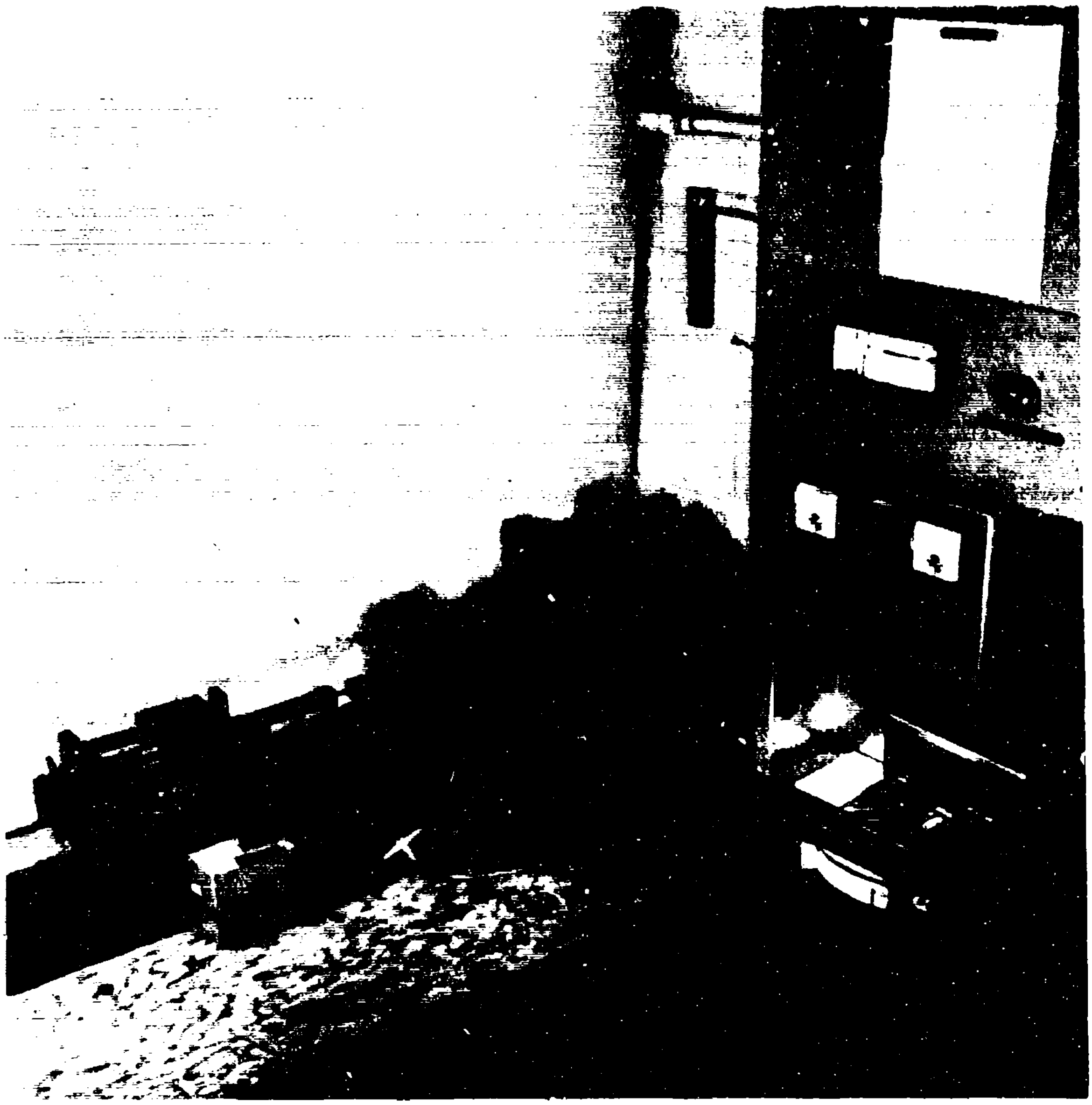

FIG. 1 TORSIONAL FATIGUE MACHINE

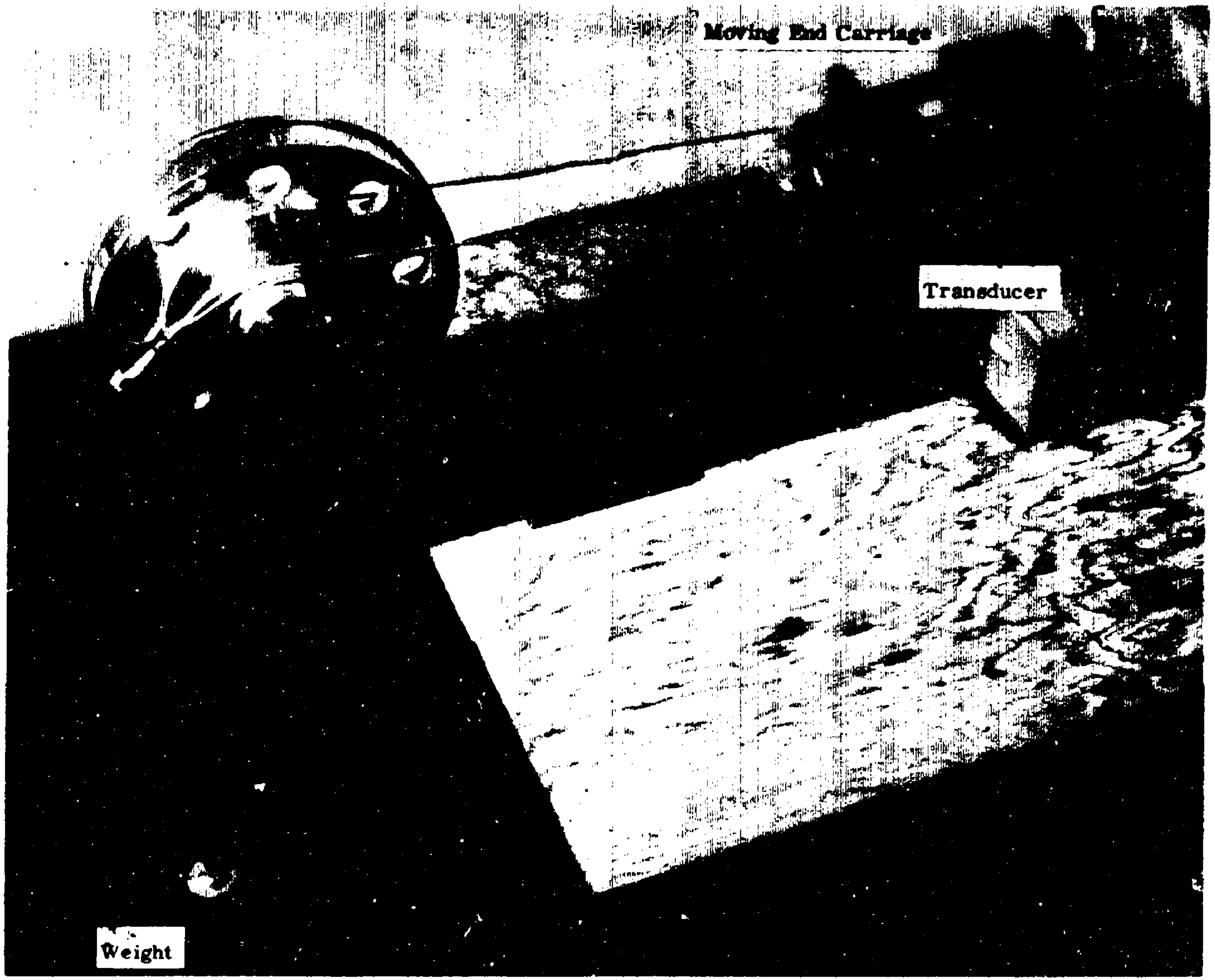

FIG. 2 TENSILE LOADING DEVICE

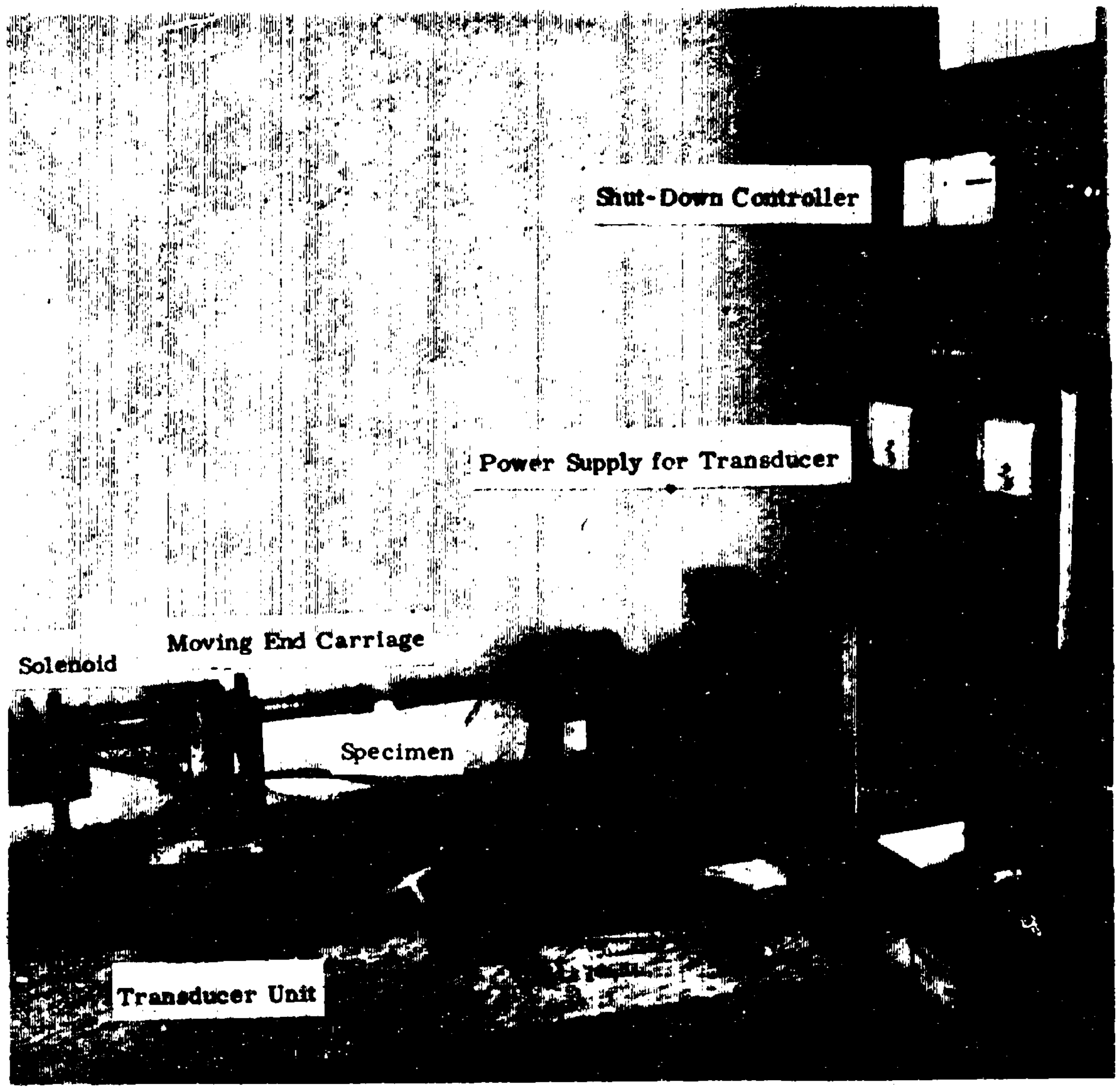

FIG. 3 AUTOMATIC SHUT-DOWN CIRCUIT

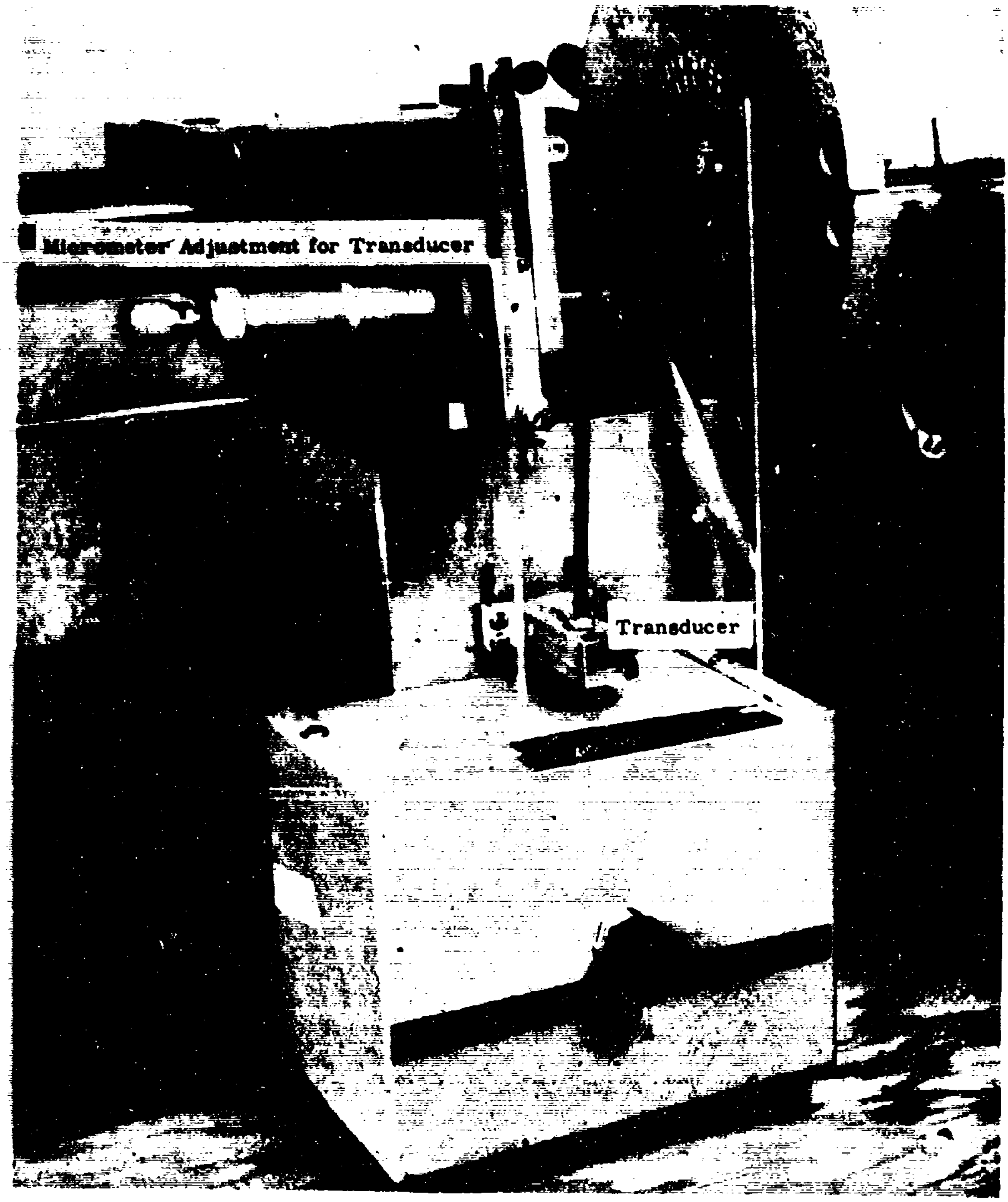

FIG. 4 TRANSDUCER

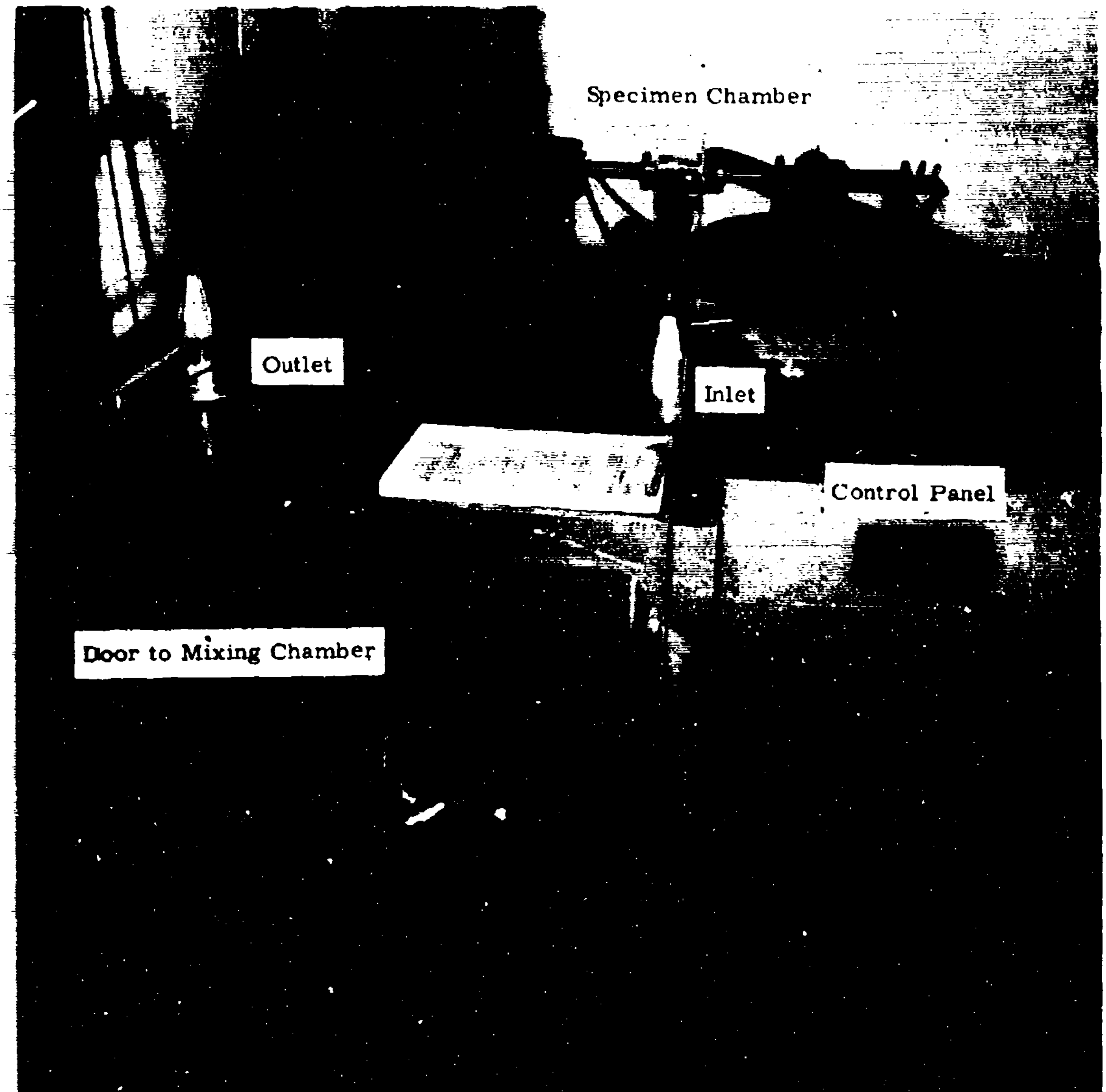

FIG. 5 HUMIDITY UNIT

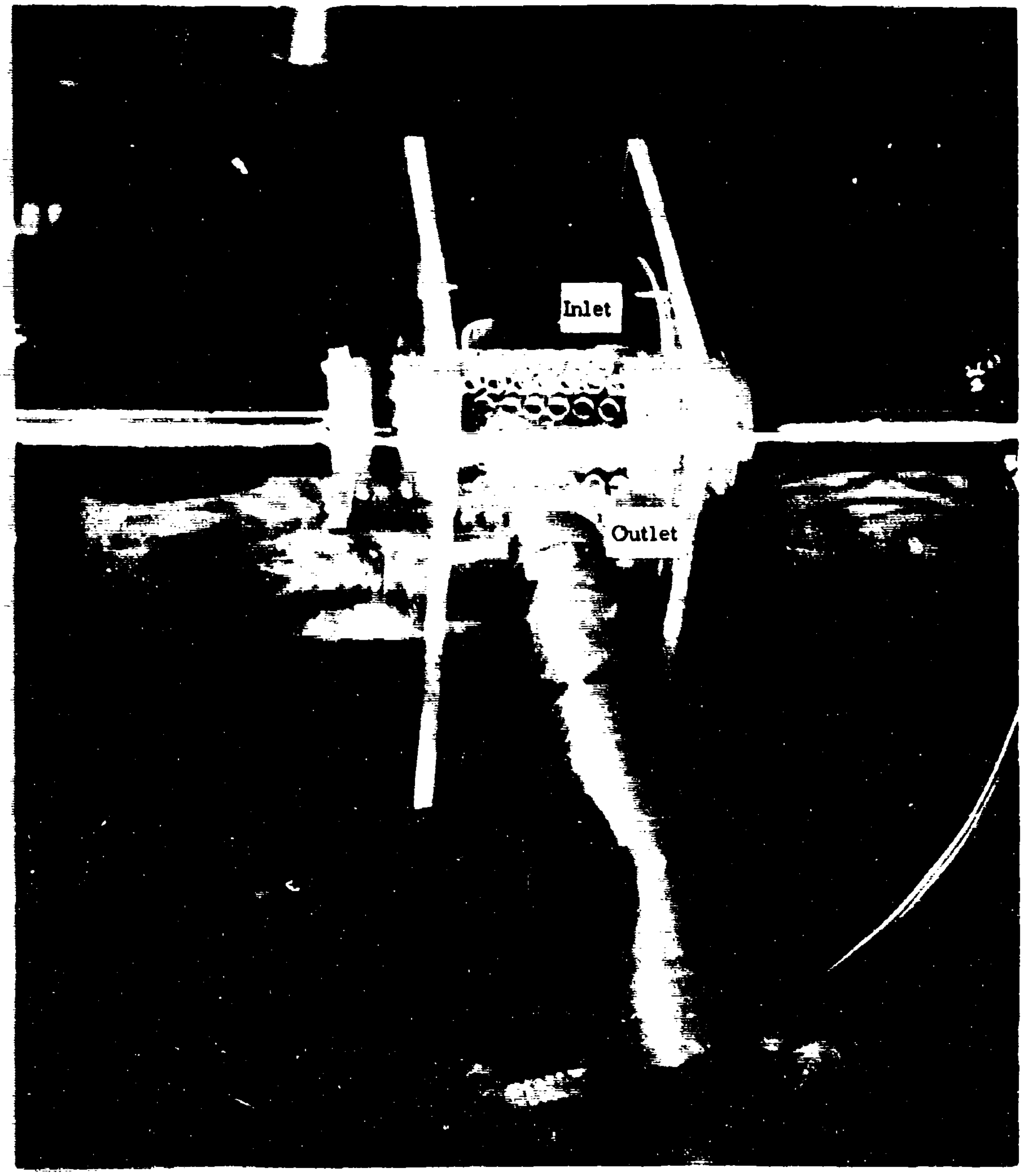

FIG. 6 HUMIDITY CHAMBER

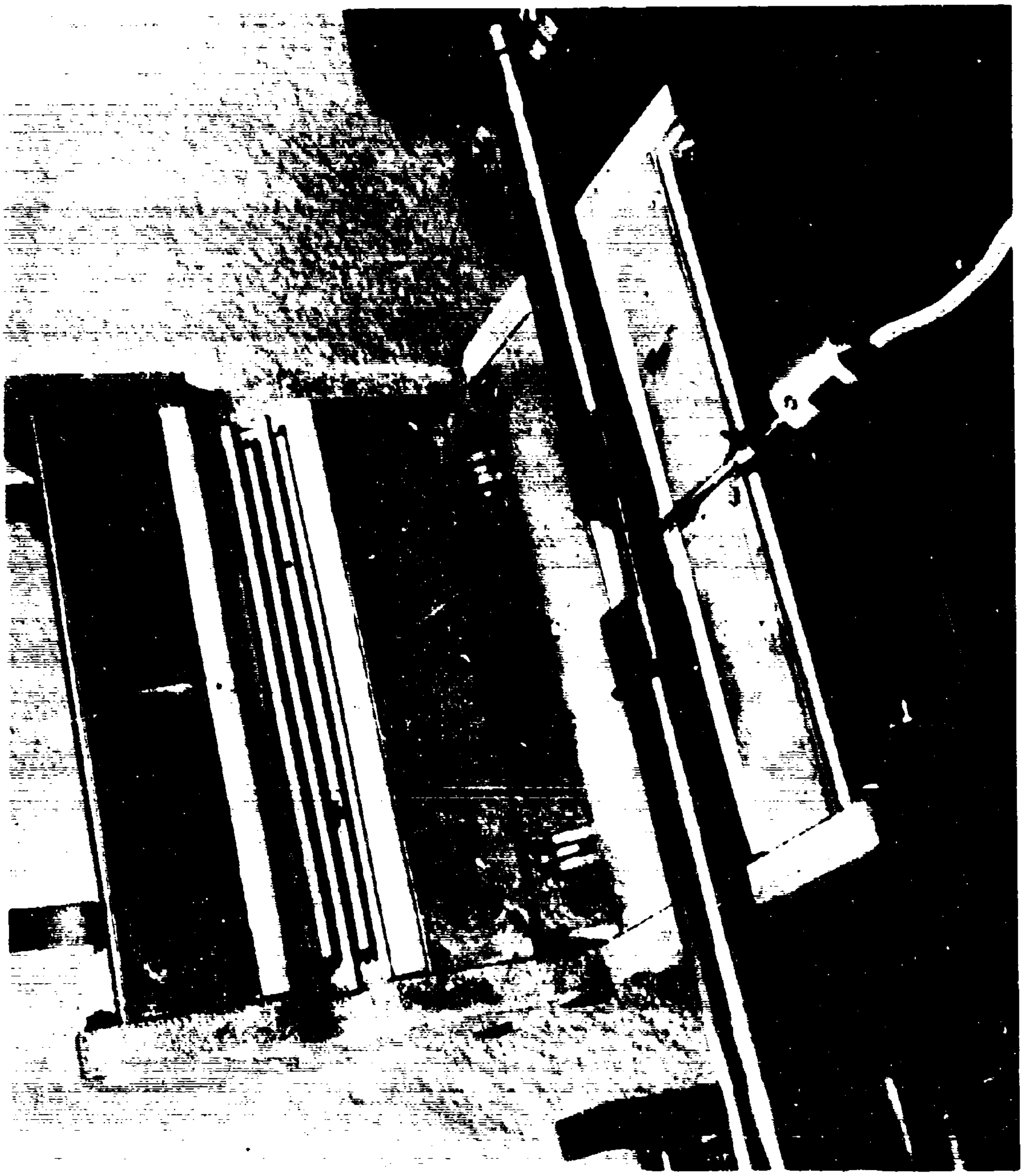

FIG. 7 SPECIMEN HEATER UNIT

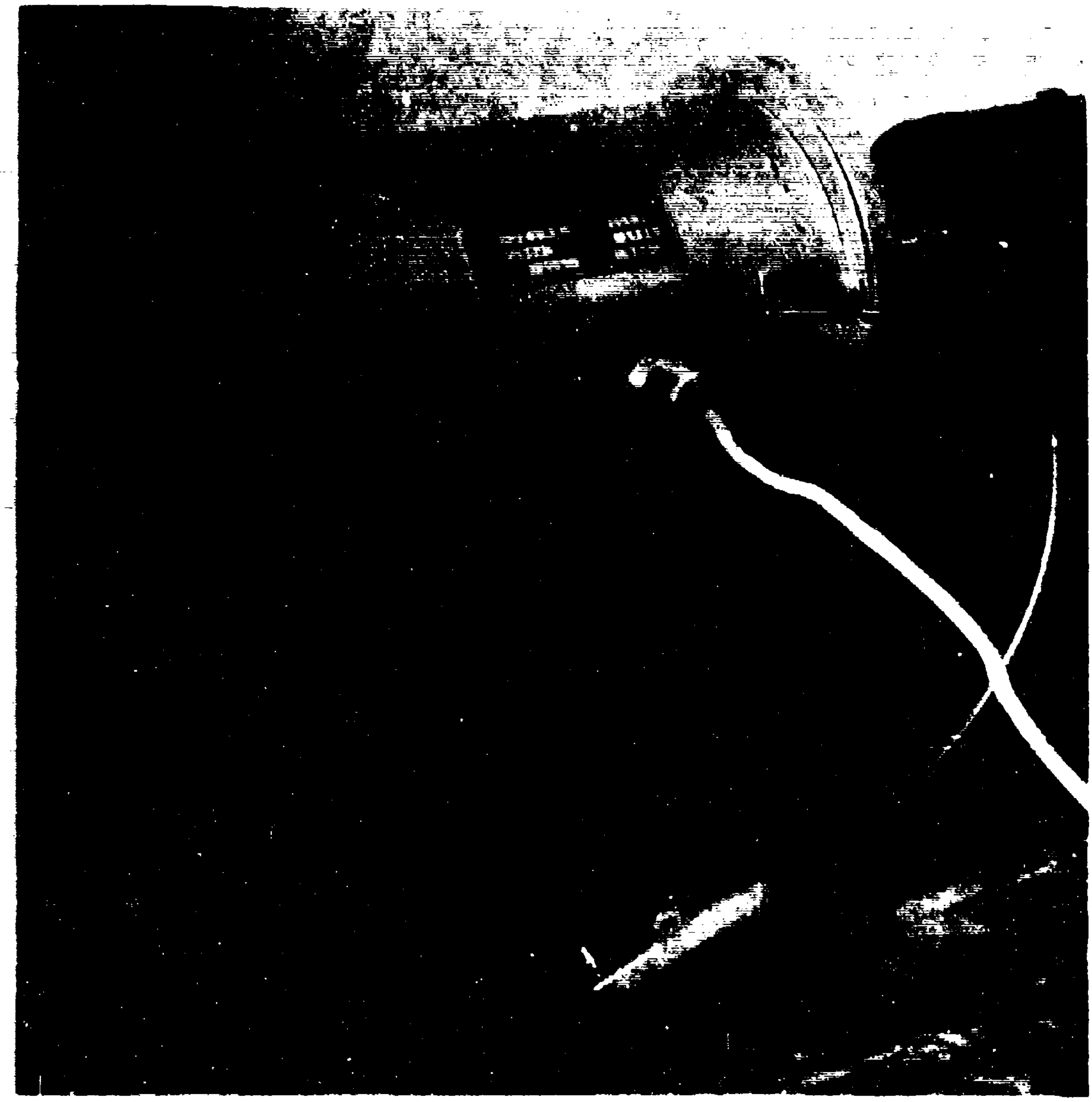

FIG. 8 SPECIMEN HEATER UNIT

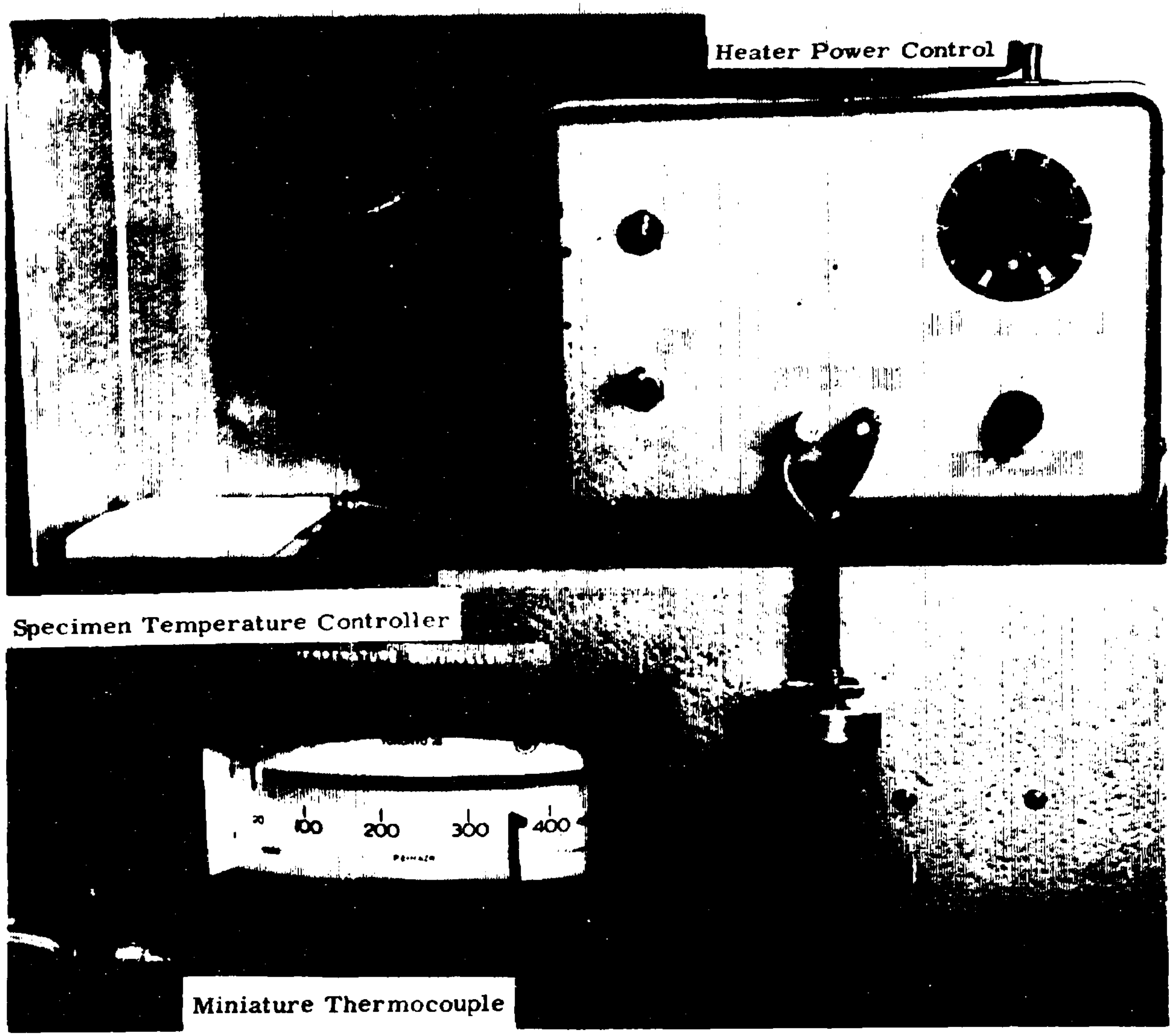

FIG. 9 SPECIMEN HEATER CONTROL UNIT

FIG. 10 GRAIN STRUCTURE, COPPER ROD AS RECEIVED, x 75

NOTE: In all micrographs, the horizontal direction of the photos coincides with the specimen axis.

FIG. 11 BACK-REFLECTION X-RAY, COPPER ROD AS RECEIVED

Fig. 12 Specimen Dimensions

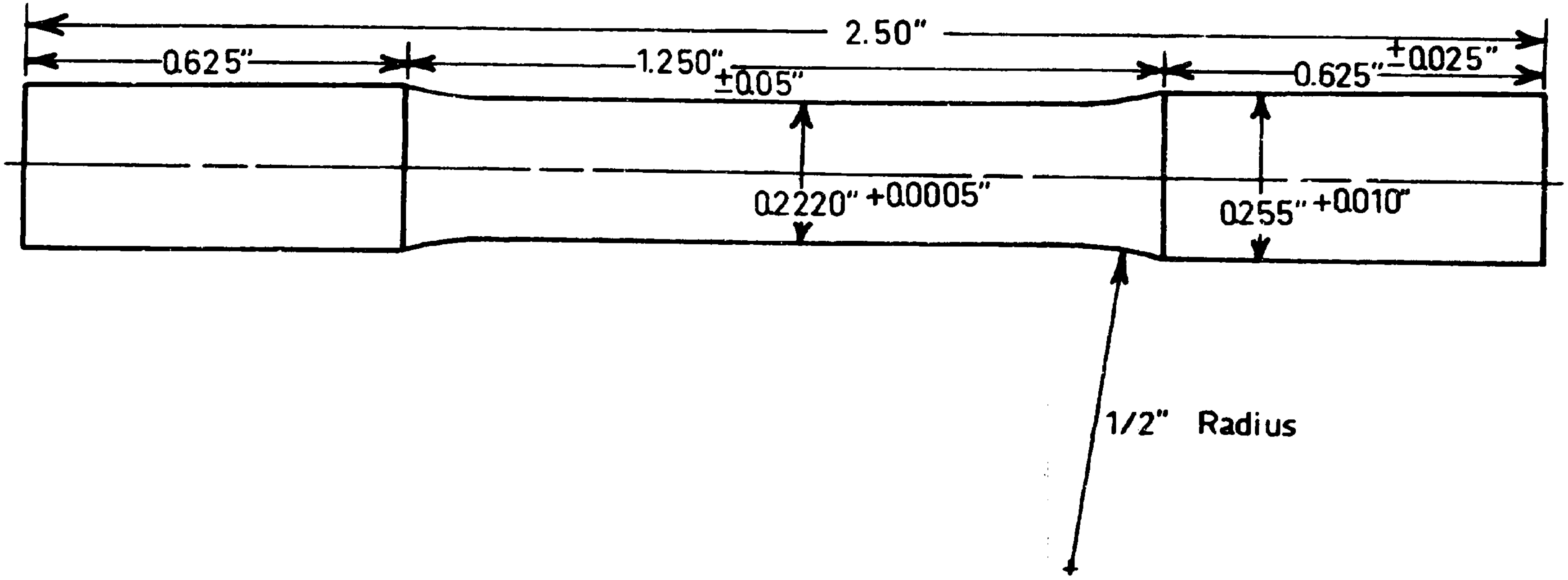

FIG. 13 ANNEALING OVEN

Fig. 14 Heating and Cooling Curve - Group A

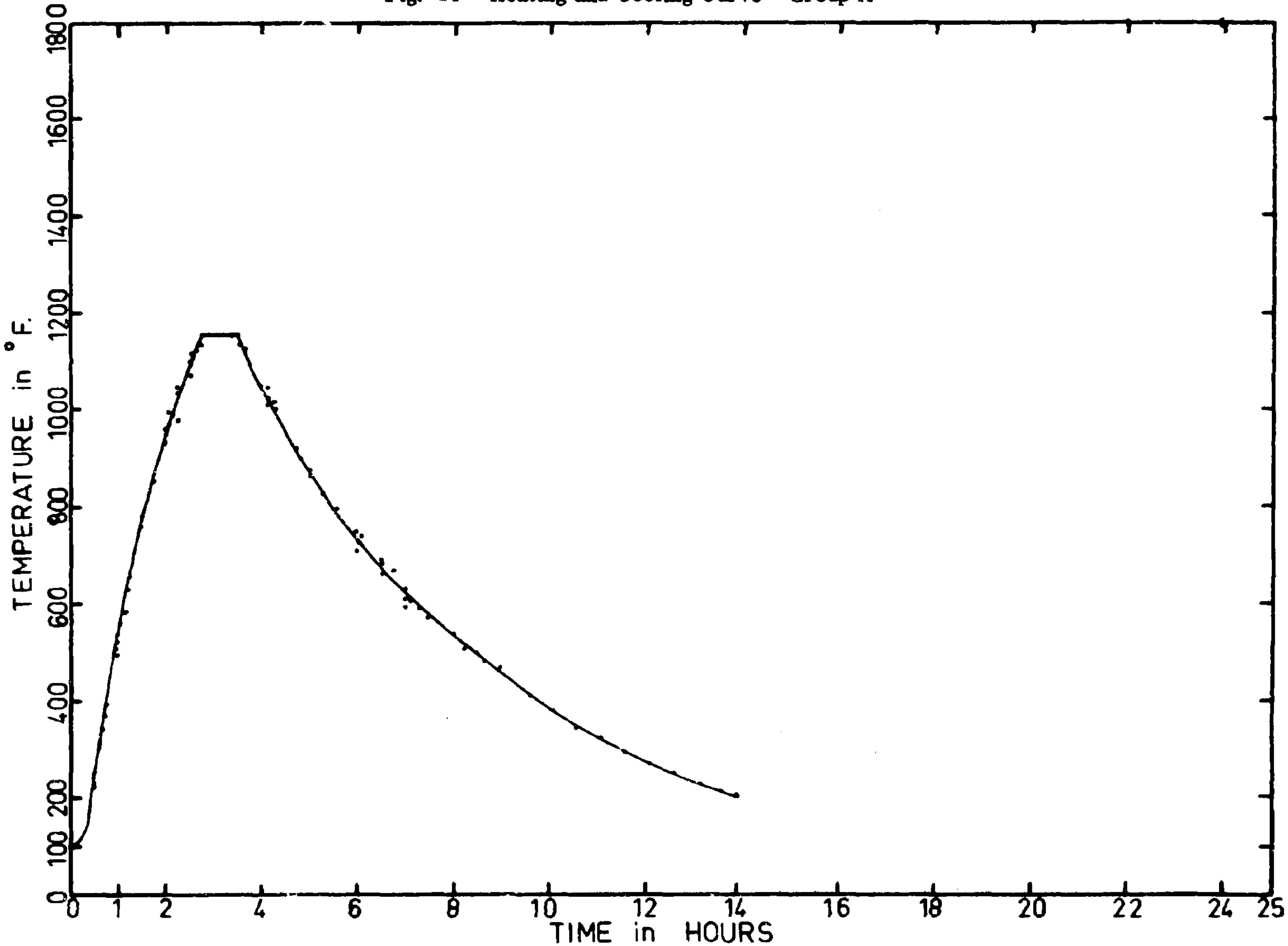

FIG. 15 GRAIN STRUCTURE, SMALL GRAINS, x 75

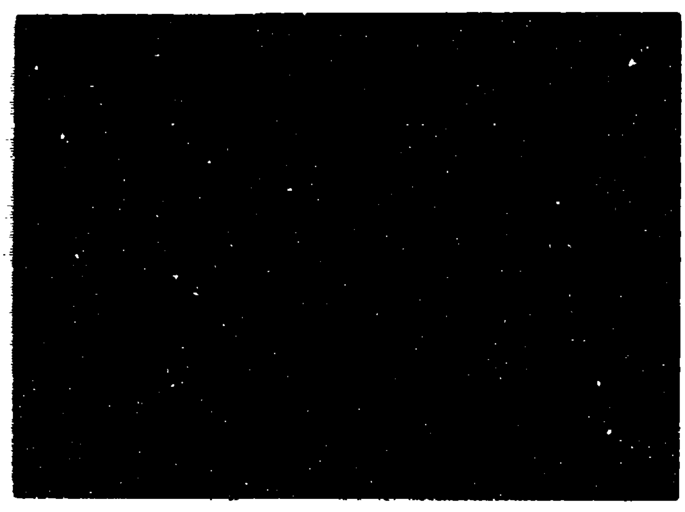

FIG. 16 BACK-REFLECTION X-RAY, SMALL GRAINS

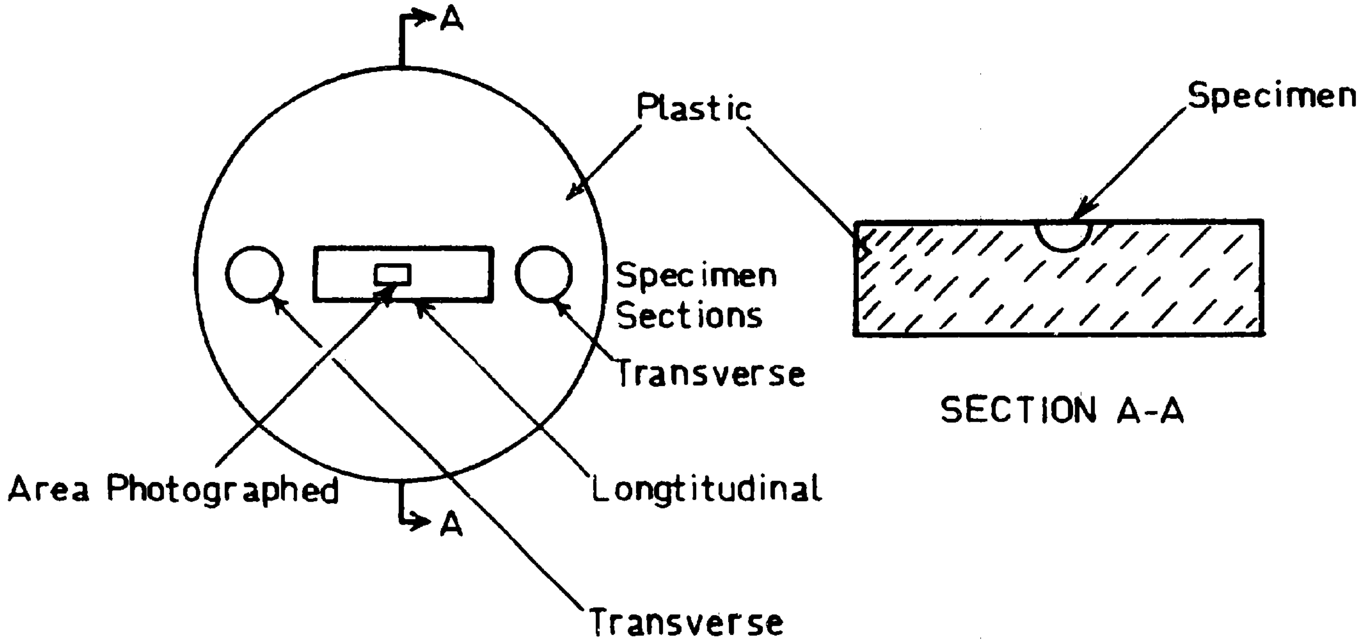

Fig. 17 Position of Photomicros of Figures 15, 19

Fig. 18 Heating and Cooling Curve - Group B

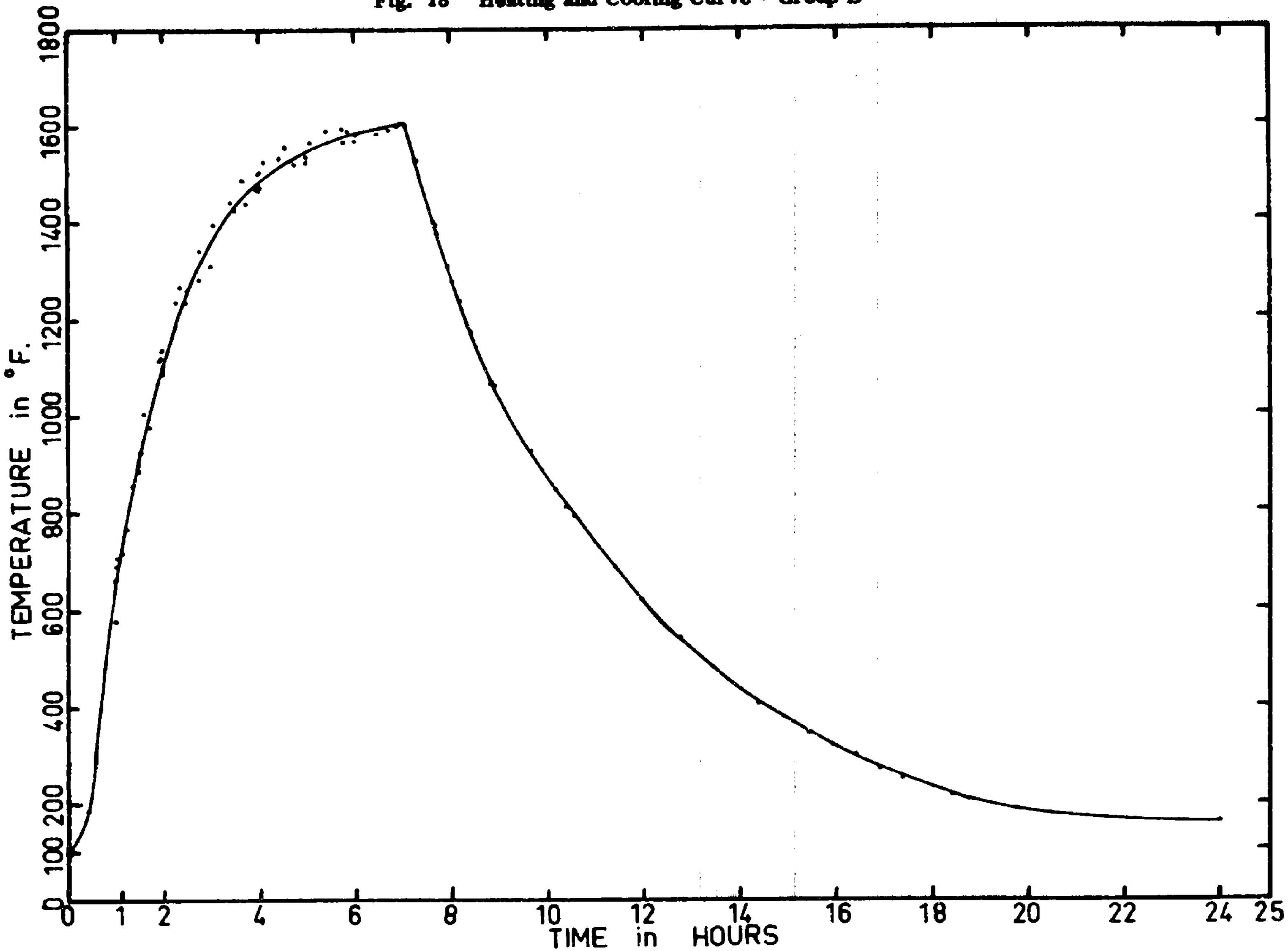

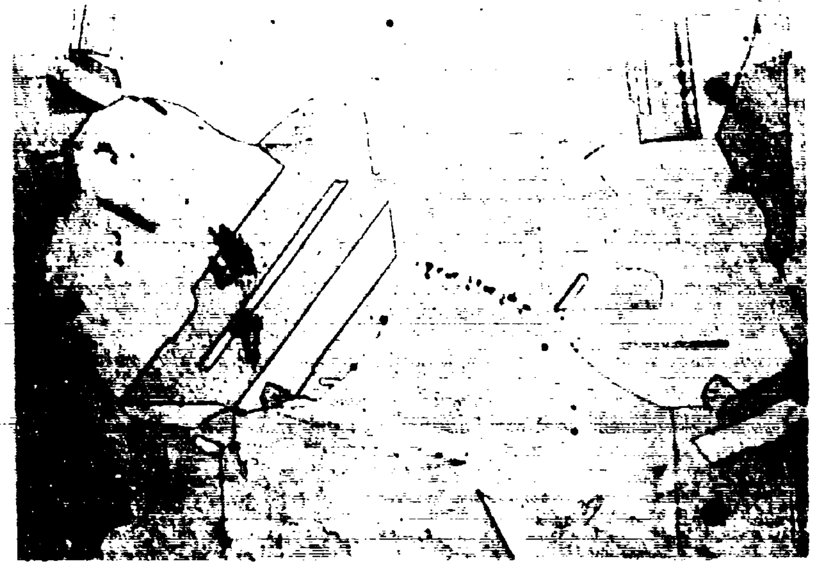

FIG. 19 GRAIN STRUCTURE, LARGE GRAINS, x 75

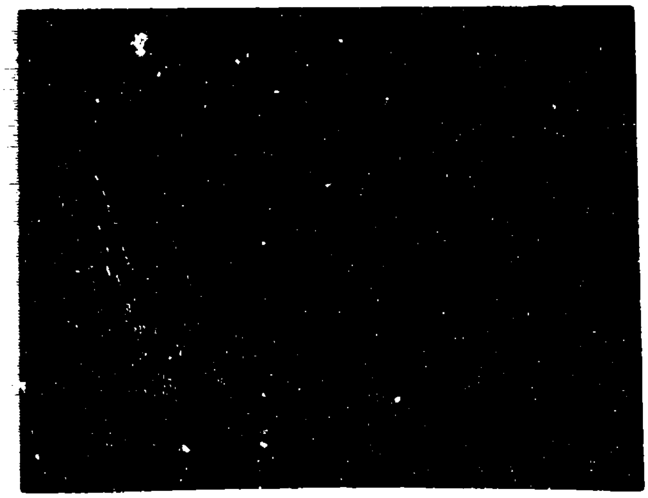

FIG. 20 BACK-REFLECTION X-RAY, LARGE GRAINS

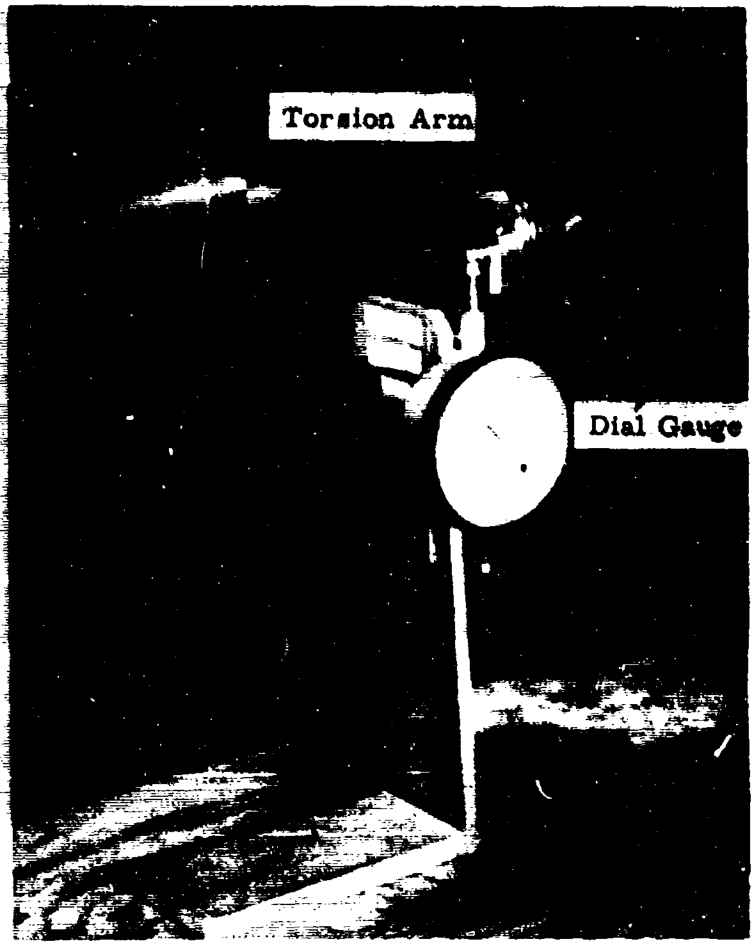

FIG. 21 DIAL GAUGE FOR ZEROING LOAD

Fig. 22 Typical Creep Curve

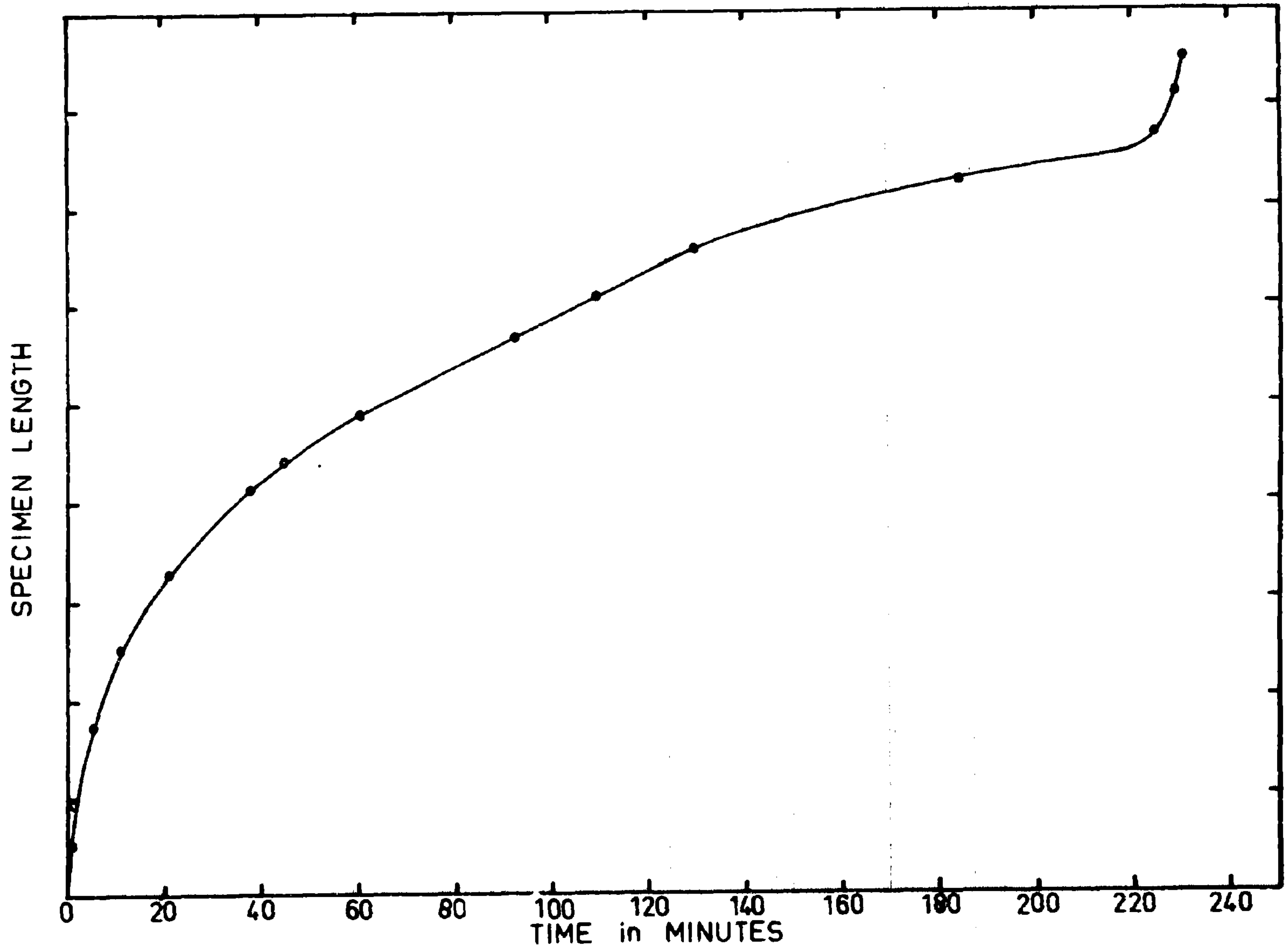

FIG. 23 - Effect of Humidity on Fatigue Life - Small Grain Size

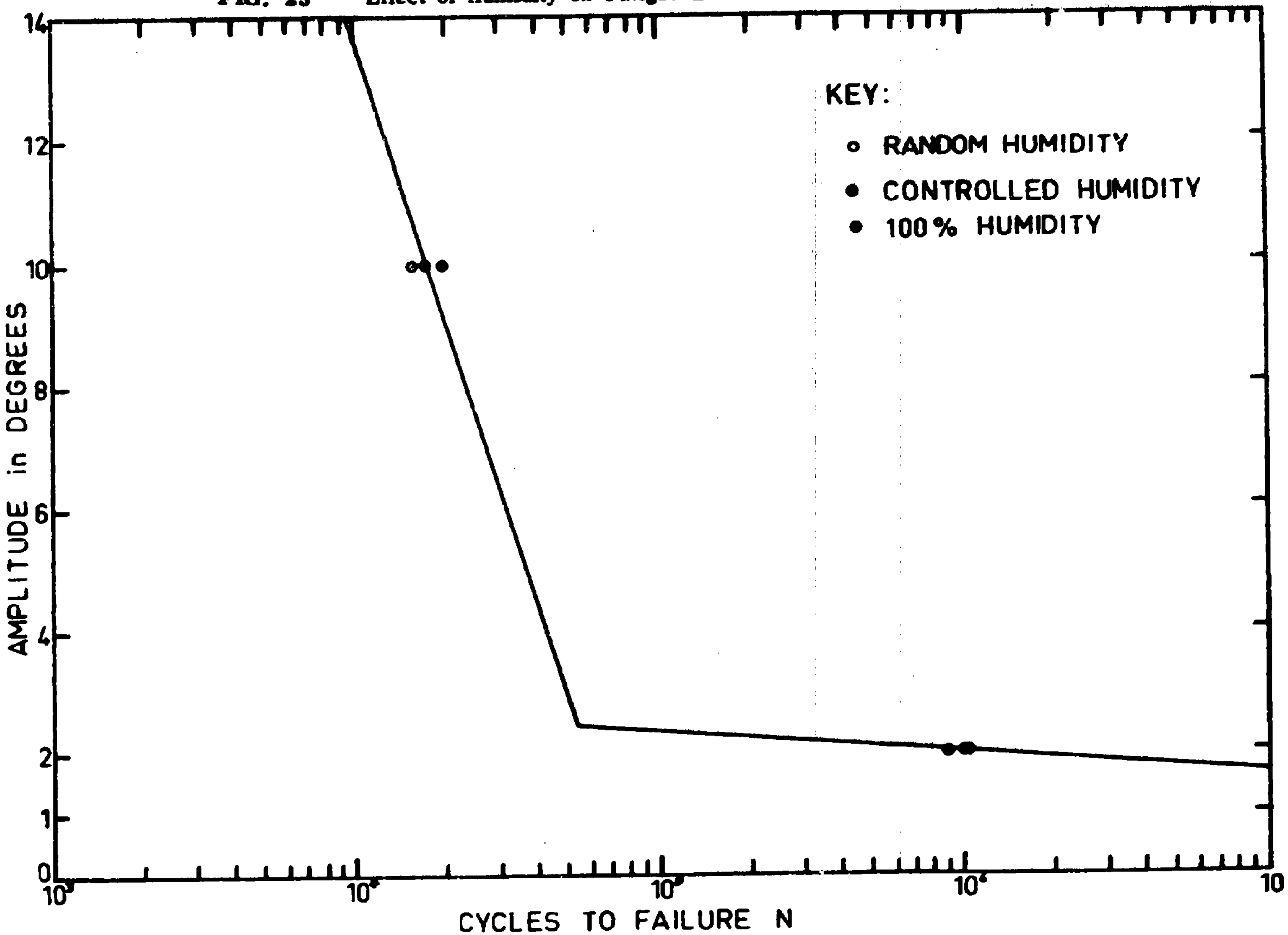

FIG. 24 Effect of Humidity on Fatigue Life - Large Grain Size

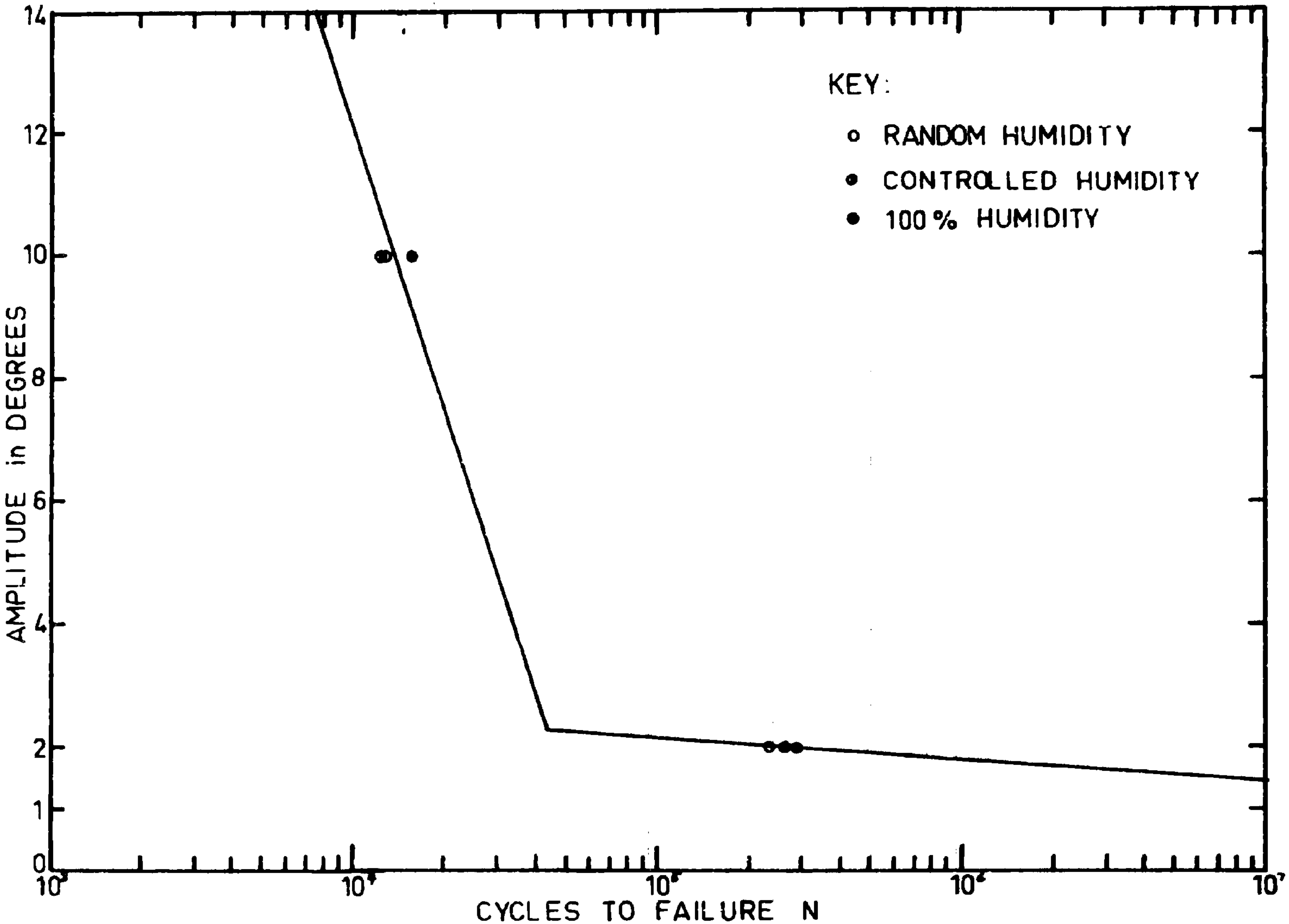

FIG. 25 Effect of Temperature on Fatigue Life - Small Grain Size

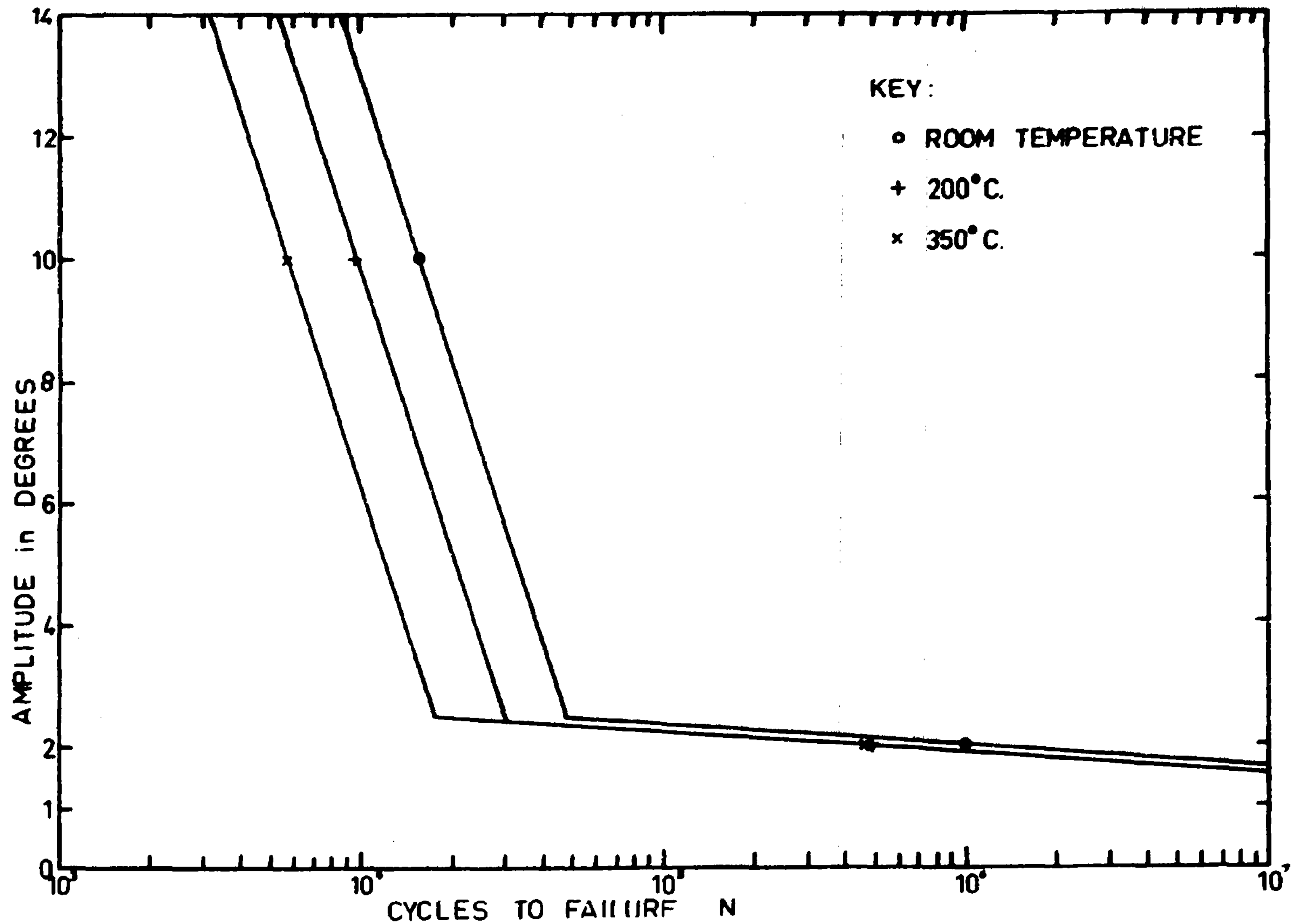

FIG. 26 Effect of Temperature on Fatigue Life - Large Grain Size

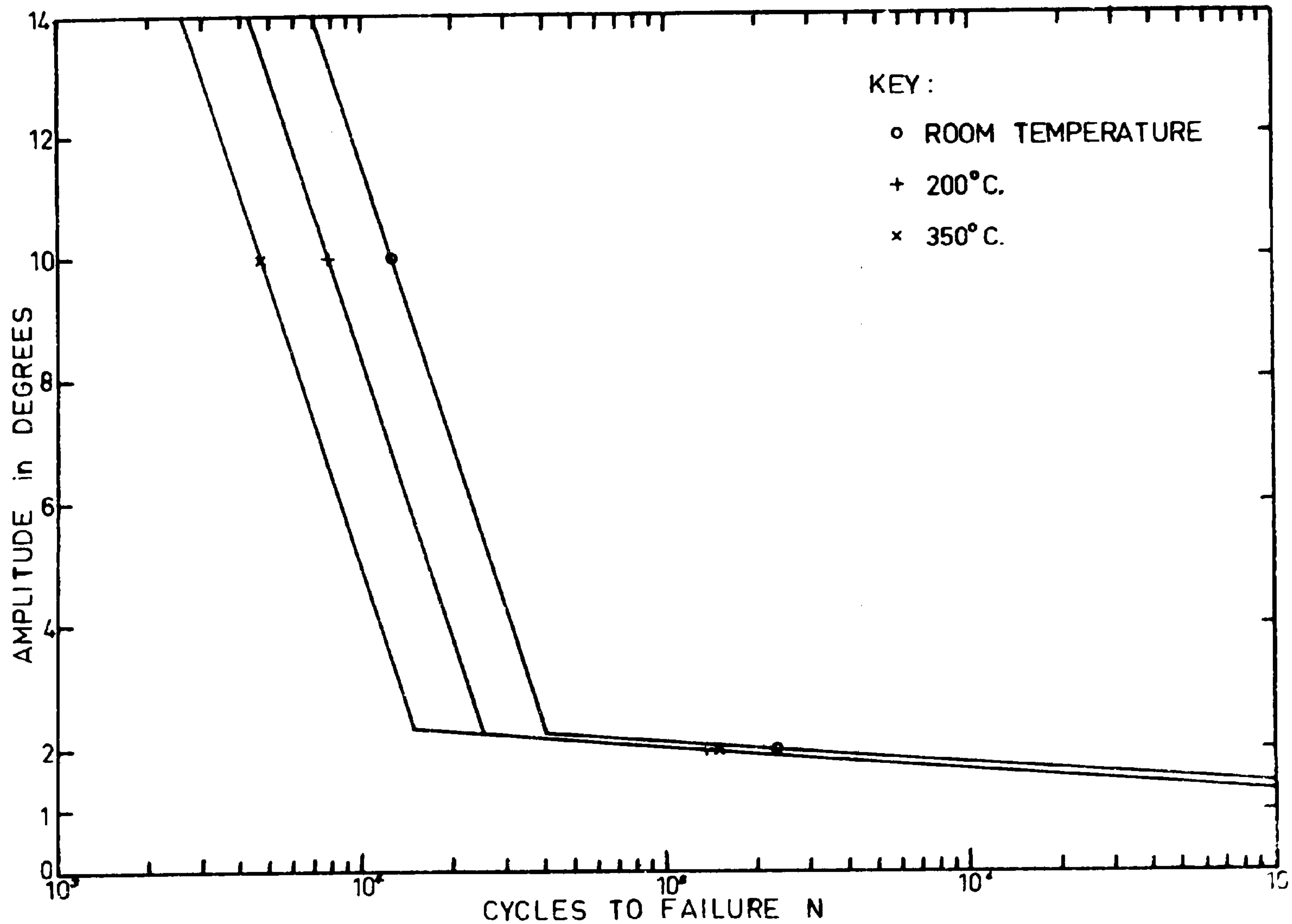

Fig. 27. Effect of Grain Size on Fatigue Life at Room Conditions

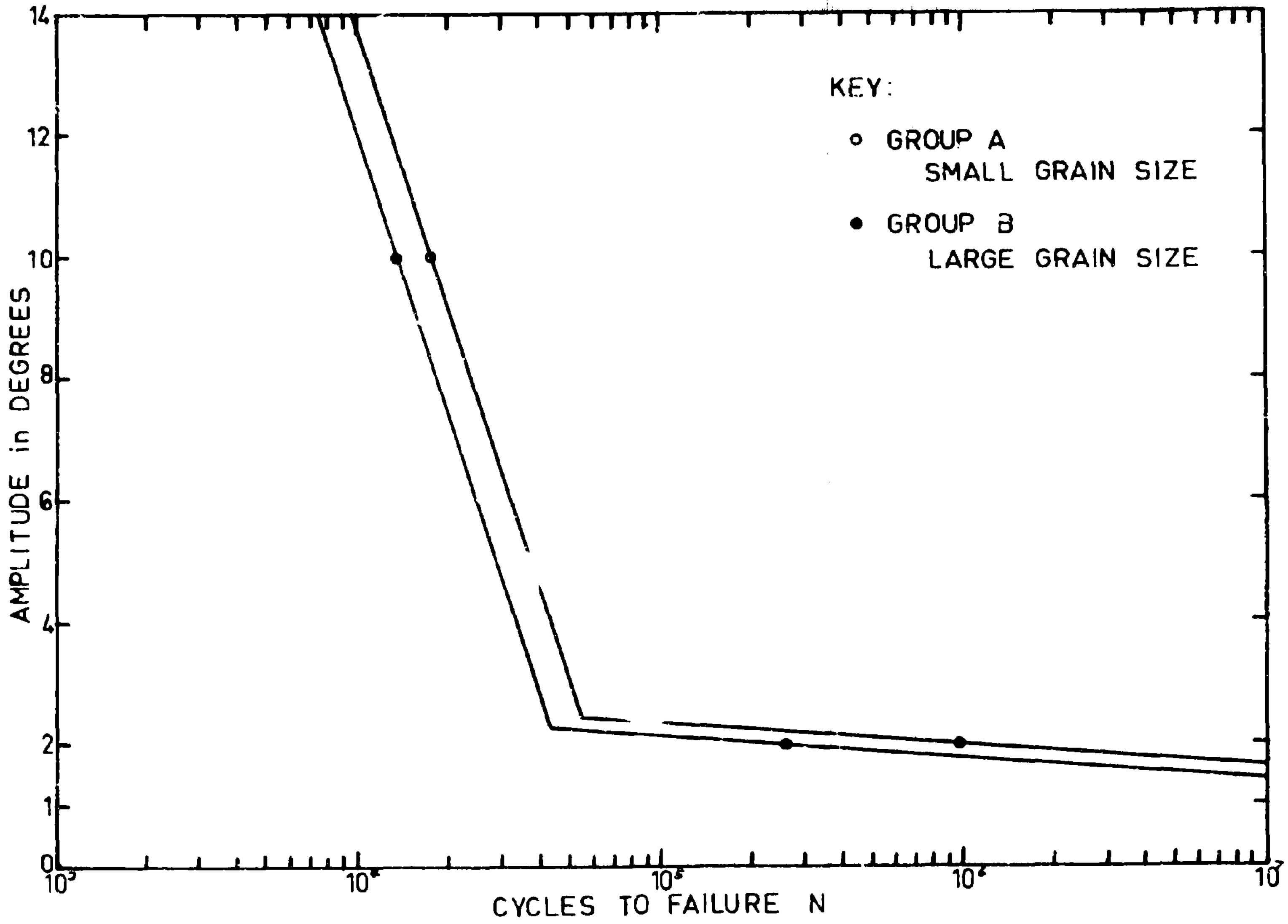

Fig. 28 Effect of Elevated Temperature Upon Fatigue Life

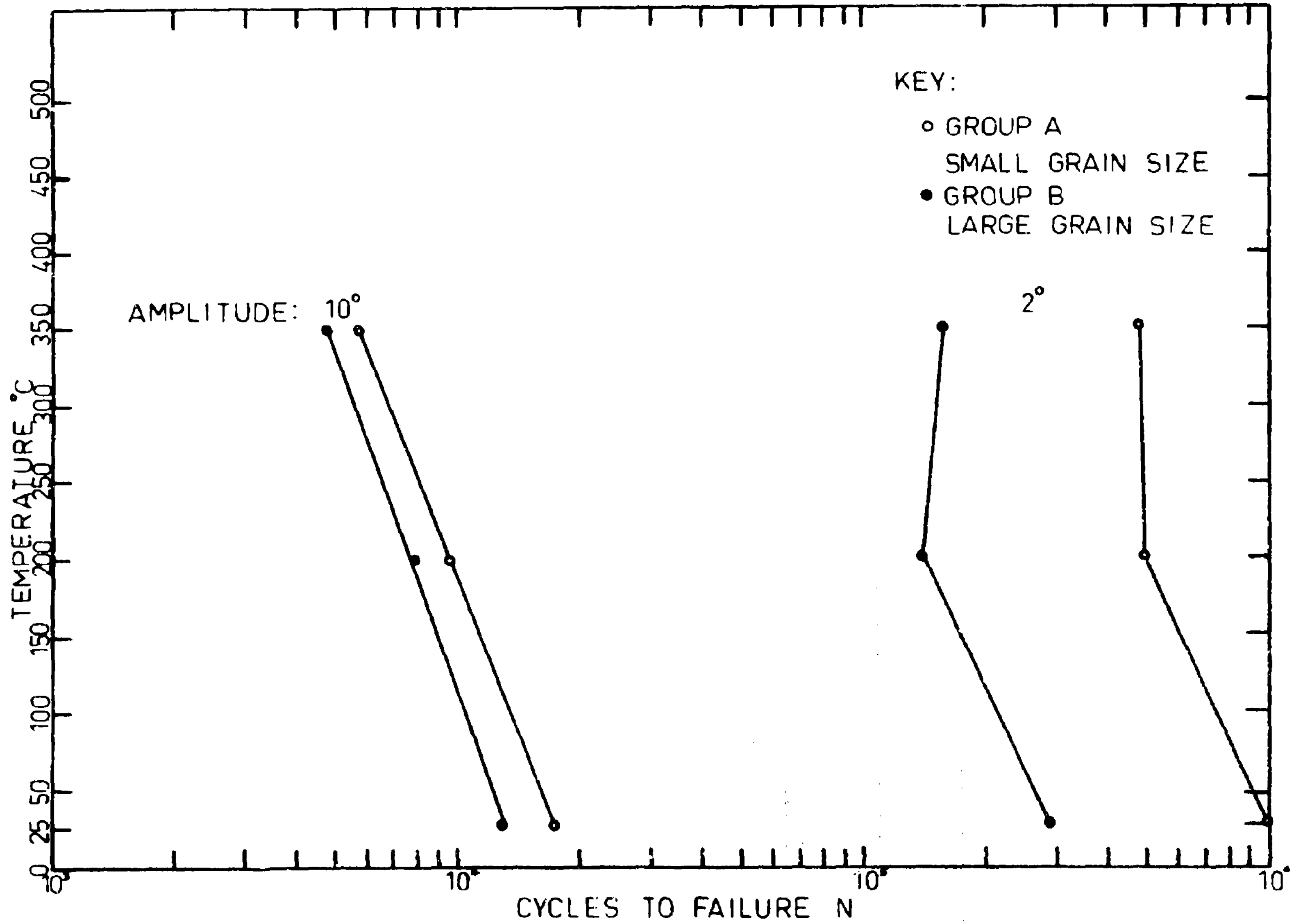

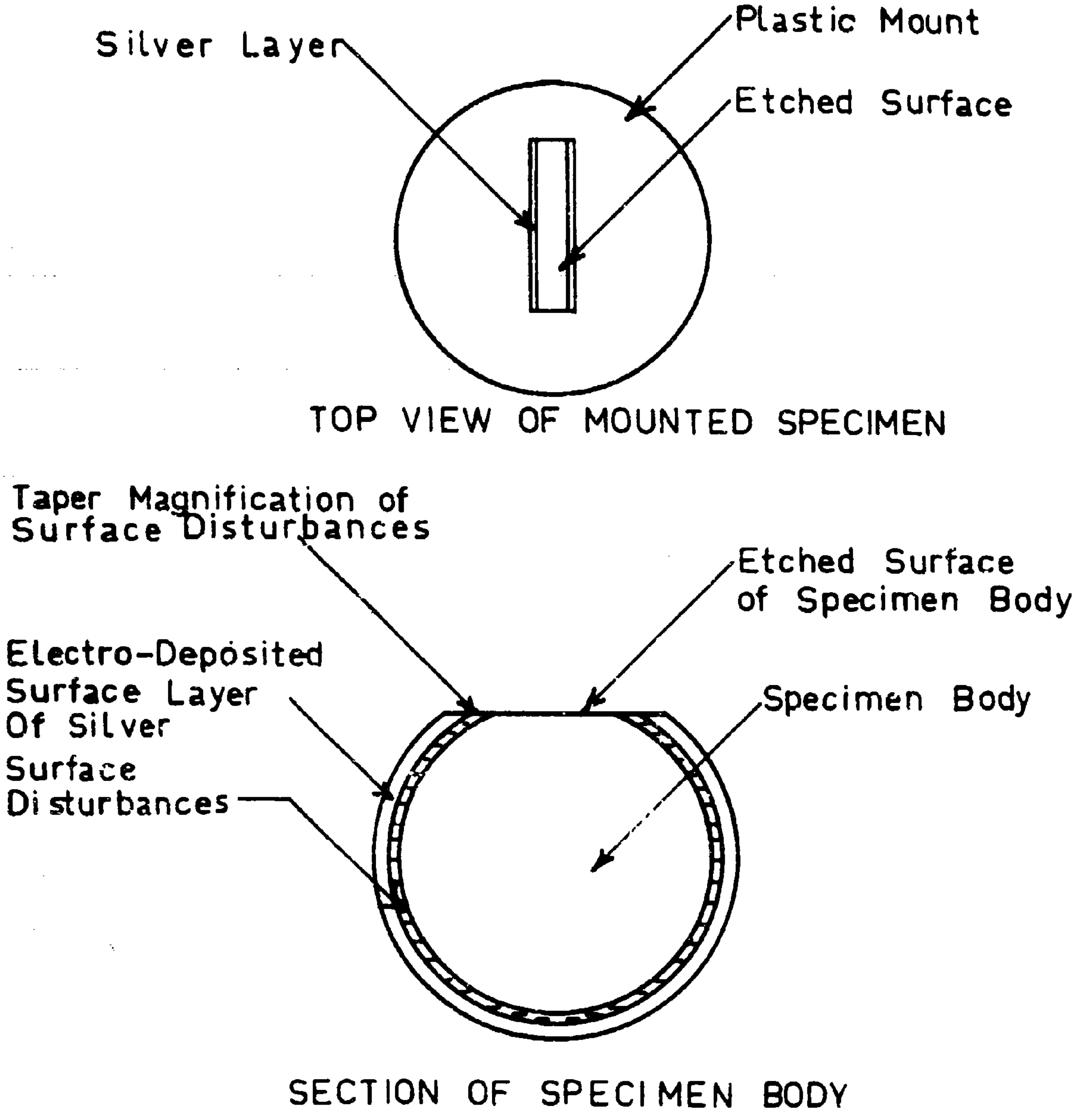

Fig. 29 Section Procedure for Photomicros

FIG. 30 FATIGUED SPECIMEN BATCH 1, SMALL GRAINS, ROOM CONDITIONS, ± 2.0 deg., x 200

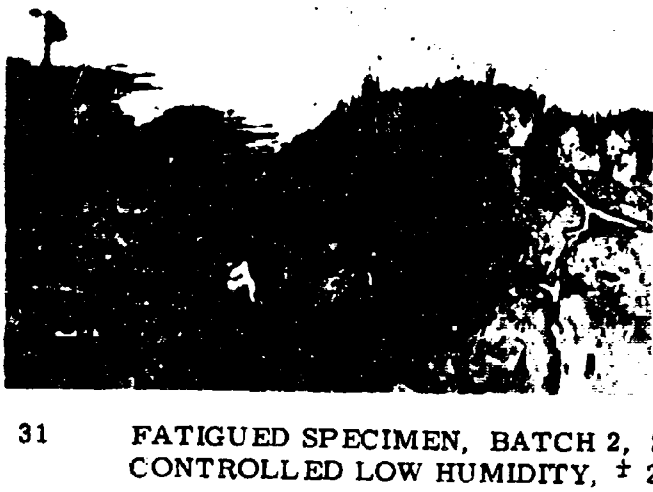

FIG. 31 FATIGUED SPECIMEN, BATCH 2, SMALL GRAINS, CONTROLLED LOW HUMIDITY, ± 2.0 deg., x 500

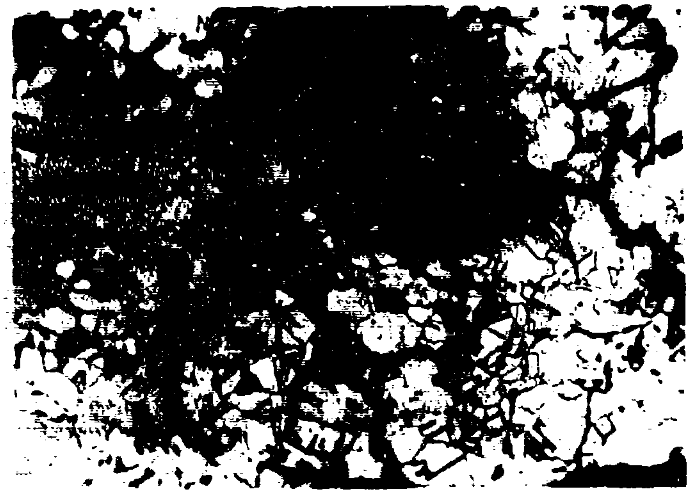

FIG. 32 FATIGUED SPECIMEN, BATCH 3, SMALL GRAINS, CONTROLLED HIGH HUMIDITY, ± 2.0 deg., x 100

FIG. 33 FATIGUED SPECIMEN, BATCH 4, SMALL GRAINS, 200°C., ± 2.0 deg., x 200

FIG. 34 FATIGUED SPECIMEN, BATCH 5, SMALL GRAINS, 350°C., ± 2.0 deg., x 200

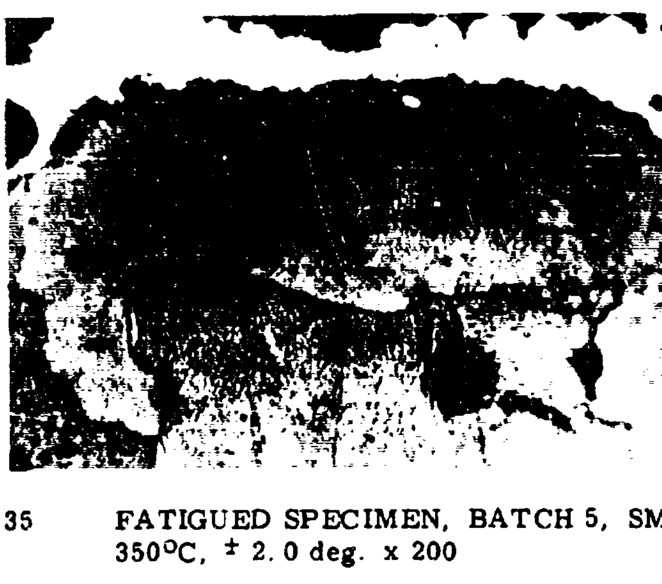

FIG. 35 FATIGUED SPECIMEN, BATCH 5, SMALL GRAINS, 350°C, ± 2.0 deg. x 200

FIG. 36 FATIGUED SPECIMEN, BATCH 6, LARGE GRAINS, ROOM CONDITIONS, ± 2.0 deg., x 100

FIG. 37 FATIGUED SPECIMEN, BATCH 7, LARGE GRAINS, CONTROLLED LOW HUMIDITY, ± 2.0 deg., x 200

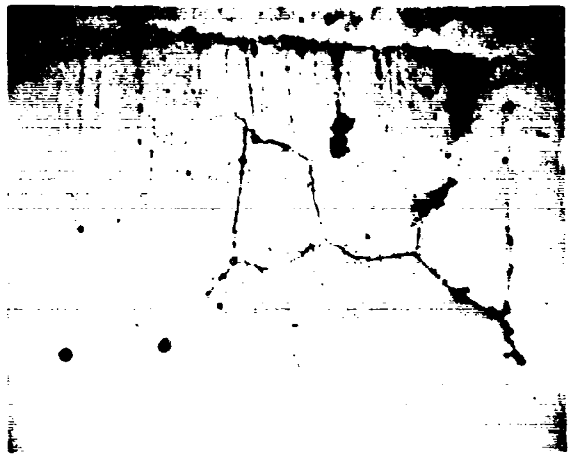

FIG. 38 FATIGUED SPECIMEN, BATCH 8, LARGE GRAINS, CONTROLLED HIGH HUMIDITY, ± 2.0 deg., x 200

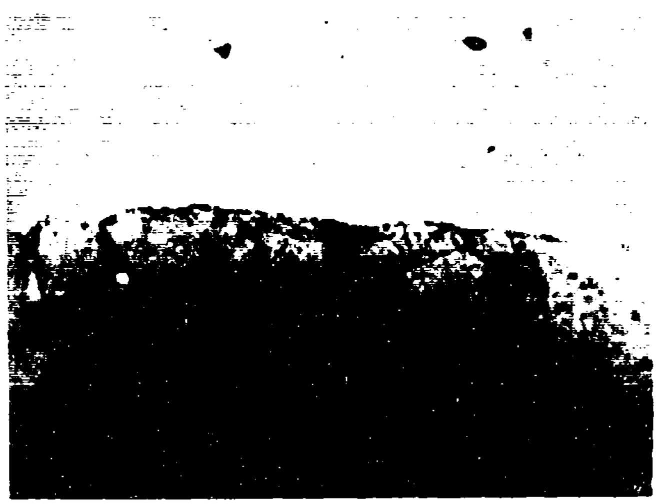

FIG. 39 FATIGUED SPECIMEN, BATCH 9, LARGE GRAINS, 200°C., ± 2.0 deg., x 200

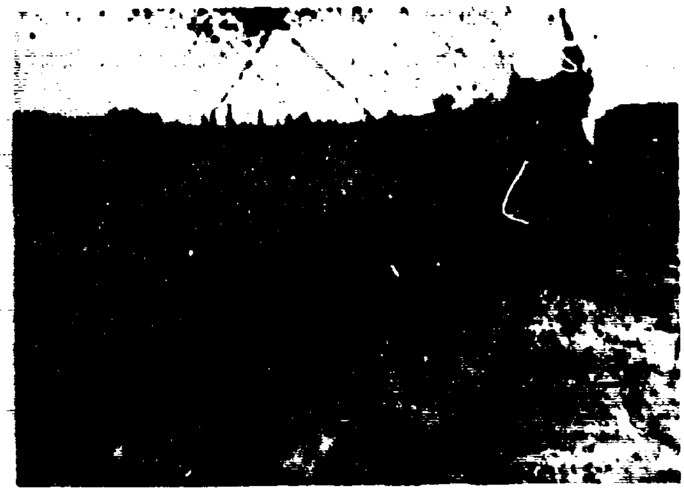

FIG. 40 FATIGUED SPECIMEN, BATCH 10, LARGE GRAINS, 350°C, ± 2.0 deg. x 200

FIG. 41 FATIGUED SPECIMEN, BATCH 11, SMALL GRAINS, ROOM CONDITIONS ± 10.0 deg., x 200

FIG. 42 FATIGUED SPECIMEN, BATCH 12, SMALL GRAINS, CONTROLLED LOW HUMIDITY, $\pm$ 10.0 deg., x 1000

FIG. 43 FATIGUED SPECIMEN, BATCH 13, SMALL GRAINS, CONTROLLED HIGH HUMIDITY, $\pm$ 10.0 deg., x 100

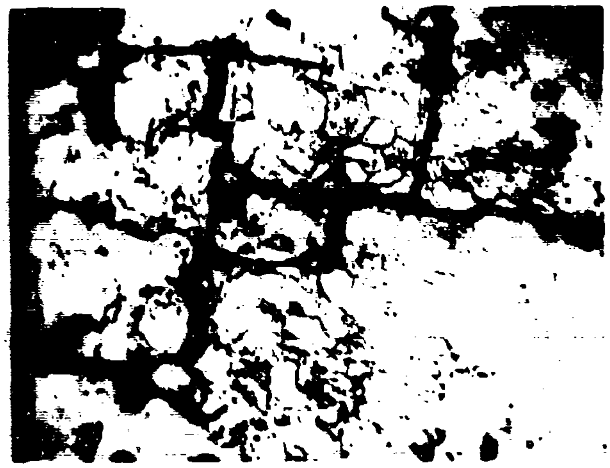

FIG. 44 FATIGUED SPECIMEN, BATCH 14, SMALL GRAINS, 200°C., ± 10.0 deg., x 200.

FIG. 45 FATIGUED SPECIMEN, BATCH 15, SMALL GRAINS, 350°C., ± 10.0 deg. x 100

FIG. 46 FATIGUED SPECIMEN, BATCH 16, LARGE GRAINS, ROOM CONDITIONS, $\pm$ 10.0 deg., x 100

FIG. 47 FATIGUED SPECIMEN, BATCH 17, LARGE GRAINS, CONTROLLED LOW HUMIDITY, $\pm$ 10.0 deg., x 200

FIG. 48 FATIGUED SPECIMEN, BATCH 18, LARGE GRAINS, CONTROLLED HIGH HUMIDITY ± 10.0 deg., x 200

F .. 49 FATIGUED SPECIMEN, BATCH 19, LARGE GRAINS, 200°C., ± 10.0 deg., x 100

FIG. 50 FATIGUED SPECIMEN, BATCH 20, LARGE GRAINS, 350^{o}C., $\pm$ 10.0 deg., x 100.